European Journal of Inorganic Chemistry

Supporting Information

Iron and Zinc Metallates Supported on Ion Exchange Resins: Synergistic Catalysts for the Solvent-Free Cyclic Carbonate Synthesis from Epoxides and CO_2

Matteo Alberti, Marta Gianelli, Nicola Panza, Dominika Zákutná, Irena Matulková, and Alessandro Caselli*

Supplementary material

Iron and Zinc Metallates Supported on Ion Exchange Resins: Synergistic Catalysts for the Solvent-free Cyclic Carbonate Synthesis from Epoxides and CO_2

Matteo Alberti,[a] Marta Gianelli,[a] Nicola Panza,[a] Dominika Zákutná,[b] Irena Matulková,[b] Alessandro Caselli*[a]

[a]Department of Chemistry, Università degli Studi di Milano and ISTM-CNR, via Golgi 19, 20133 Milano, Italy. E-mail: alessandro.caselli@unimi.it; phone: +39 02 50314372.

[b]Department of Inorganic Chemistry, Charles University, Hlavova 2030/8 128 40, Prague 2, Czech Republic

*Correspondence: Alessandro Caselli
alessandro.caselli@unimi.it

TABLE OF CONTENTS

General considerations

All chemicals and solvents were commercially available and used as received except where specified. ^{1}H NMR analyses were performed with 400 MHz spectrometers at room temperature. The coupling constants (*J*) are expressed in hertz (Hz), and the chemical shifts (δ) in ppm. Catalytic tests were analysed by gas chromatography. GC-FAST technique was performed using a Shimadzu GC-2010 equipped with a Supelco SLBTM-5ms capillary column. ICP-OES elemental analyses were recorded in the analytical laboratories of Università degli Studi di Milano. SEM images and EDX spectra were acquired with a scanning electron microscope (SEM) Jeol JSM-5500 LV. The Raman spectra were measured at several (three) random positions to demonstrate the homogeneity of sample. The Raman spectra were recorded on a Thermo Scientific DXR Raman Microscope interfaced to an Olympus microscope (objectives 50x) using a depolarized 532 and 780 nm frequency-stabilized single mode laser (0.1–5 mW for 532 nm and 15-24 mW for 780 nm laser power, approx. 30–1874 cm^{-1} and 25–1877 cm^{-1}) spectral range, 1800 and 830 lines/mm grating, for 532 and 780 nm wavelength, respectively). The spectrometer was calibrated using a software-controlled calibration procedure employing multiple neon emission lines (wavelength calibration), multiple polystyrene Raman bands (laser frequency calibration) and standardized white light sources (intensity calibration). Magnetization measurements were performed at a physical property measurement system (PPMS) from Quantum Design equipped with a Vibrating Sample Magnetometry (VSM) module. All CO_2 cycloaddition reactions were carried out in a 300 mL steel Parr autoclave, with standard autoclave glass vials, capped with a septum. The reactions were performed in solvent-free conditions and on 500 mg of substrate, unless otherwise stated. The optimization of the reaction was designed with Stat-Ease 360 Software.

Functionalization and characterization of ion exchange resins

General procedure for resin conditioning

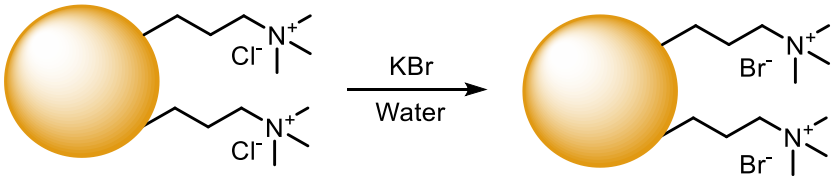

50 g of Amberlite™ IRA-400 (**IRA400**) or Amberlyst™ A26 (**A26**) resins, both in Cl^- form, were packed into a Versaflash™ solid sample loading cartridge. 250 mL of a 20% wt KBr aqueous solution were then recirculated for 4 hours at a 50 mL/min rate. 1 L of distilled water was then flushed to clean the resin from excess KBr. The obtained resins (**IRA-400-Br** and **A26-Br**) were then filtered, and bromide exchange was verified with EDS spectroscopy (Figure S 1 and Figure S 2). The resins were then used for further functionalization.

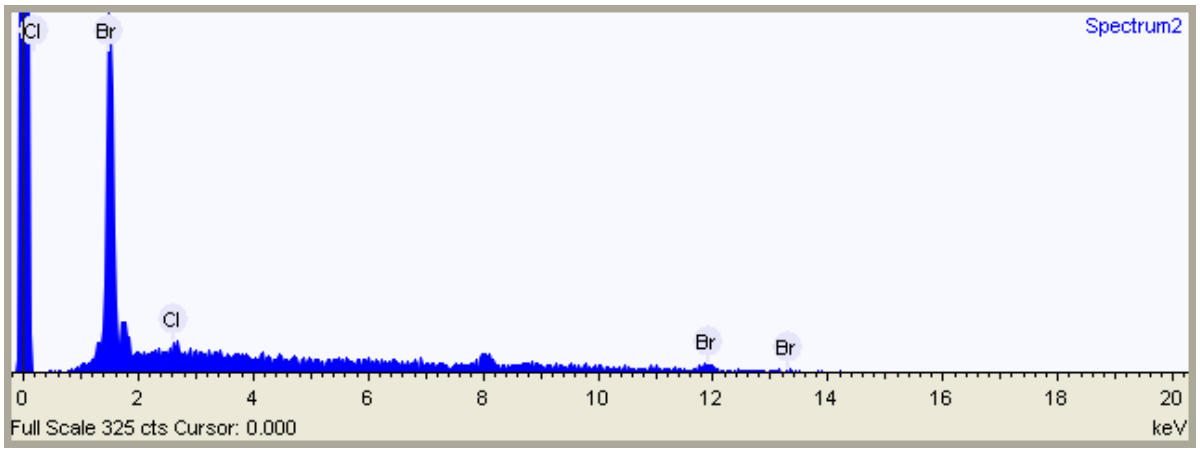

Figure S 1: SEM-EDS spectrum of ***IRA-400-Br***

Element	Weight %
Chlorine	3.3
Bromine	96.7

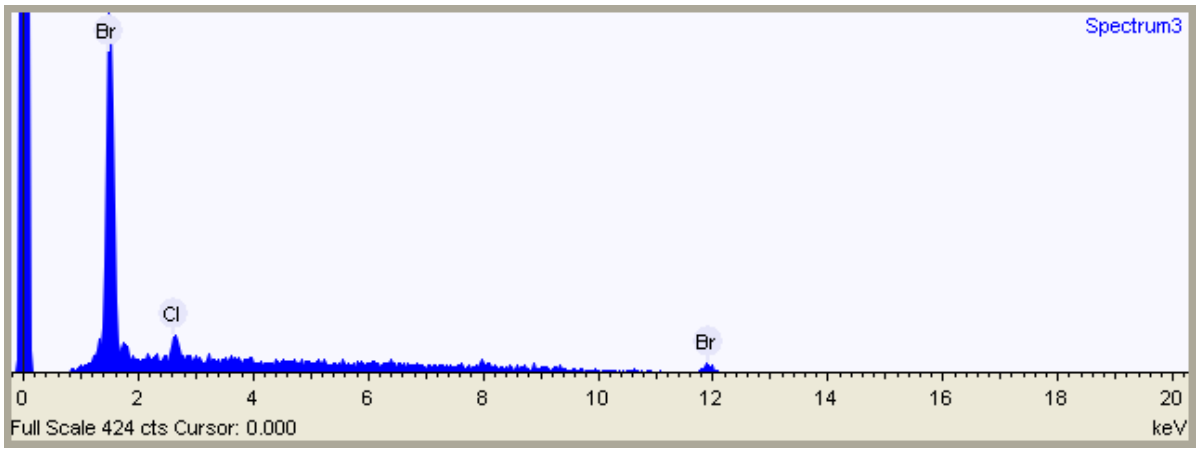

Figure S 2: SEM-EDS spectrum of ***A26-Br***

Element	Weight %
Chlorine	6.9
Bromine	93.1

Acquisition conditions

Acquisition time (s) 90.0
Process time 4
Accelerating voltage (kV) 15.0

Metalation with iron chloride

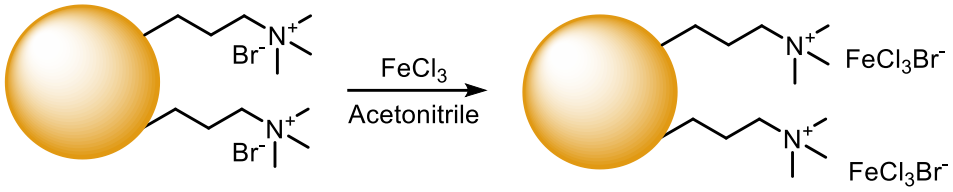

2a, IRA-400 $FeCl_3Br$
2b, A26 $FeCl_3Br$

4 mL of **IRA-400-Br** or **A26-Br** were poured into test tubes containing a 10 mL solution of iron chloride (anhydrous) in acetonitrile. The necessary iron chloride mass was calculated based on the maximum theoretical capacity of each resin:

- **IRA-400**: 1.4 meq/mL, which converts into 227.08 mg/mL of iron chloride (908 mg).
- **A26**: 0.8 meq/mL, which converts into 129.76 mg/mL of iron chloride (519 mg).

Immediately after the addition of the resins, a discoloration of the solution was observed. The tubes were then placed onto a vibromechanical agitator overnight. The resins were filtered and washed 5 times with 10 mL of acetonitrile and 3 times with 10 mL of dichloromethane. To avoid pores' collapse, the resins were not dried under vacuum. The products were then analyzed with SEM-EDS spectroscopy to evaluate correct metalation (Figure S 3 and Figure S 5) while the Fe mass content was assessed with ICP-OES (Table S 1).

Table S 1: Fe mass content in supported ferrates. Determined by ICP-OES

Resin	Wt% Fe
2a, IRA-400 $FeCl_3Br$	4.45%
2b, A26 $FeCl_3Br$	4.48%

Magnetization measurements: derivation of iron percentage

The molar susceptibility is related to the obtained magnetization by eq. 1:

$$\chi_M = \frac{M \cdot 4\pi}{H \cdot n} \tag{1}$$

with $[M] = \mathrm{emu}$, the measured magnetization, $[H] = \mathrm{Oe}$, the applied magnetic field, $[n] = \mathrm{mol}$. Because in the raw data the magnetization is measured in memu and the magnetic field in T (Tesla), in fact the conversion formula is the following (eq. 2):

$$\chi_M = \frac{M \cdot 10^{-3} \cdot 4\pi}{H \cdot 10^4 \cdot n} \tag{2}$$

Subsequently, in *non-ideal* paramagnets the molar susceptibility temperature dependence is defined by the Curie-Weiss law (eq. 3):

$$\chi_M = \frac{\mu_0 N_A \mu_{eff}^2 \mu_B^2}{3k_B(T - \theta_{CW})} \tag{3}$$

with the permeability of vacuum, μ_0, Avogadro's number, N_A, effective magnetic moment, μ_{eff}, Bohr magneton, μ_B, Boltzmann's constant, k_B, and Curie-Weiss temperature, θ_{CW}. In d-ions, where the orbital momentum is quenched due to the strong inhomogeneous electric field, the effective magnetic moment is arising only from the electron spin:

$$\mu_{eff} = 2 \cdot \sqrt{S(S+1)} \tag{4}$$

For Fe^{3+} ions in high spin state, $\mu_{eff}\left(S = \frac{5}{2}\right) = 5.91\ \mu_B$. Eq. 2 and eq. 3 can be joined in eq. 5:

$$\frac{M \cdot 10^{-3} \cdot 4\pi}{H \cdot 10^{4} \cdot n} = \frac{\mu_0 N_A \mu_{eff}^2 \mu_B^2 \cdot 10^6}{3k_B(T - \theta_{CW})} \quad (5)$$

The 10^6 factor was added to convert from CGS to SI units. Rearranging:

$$\frac{1}{M} = \frac{3k_B \cdot 4\pi}{\mu_{eff}^2 \mu_B^2 \mu_0 N_A n H \cdot 10^{13}} (T - \theta_{CW}) \quad (6)$$

$1/M$ can be plotted with T, and from the angular coefficient, n can be obtained. It can then be multiplied for the iron atomic mass and divided for the mass of the sample to obtain the weight fraction of iron in the samples. Using this method, the obtained iron content is reported in Table S 2.

Table S 2: Iron mass content for the resins, measured with magnetometry

Sample	Found moles (mol)	Sample weight (mg)	Fe, $\%_{wt}$
2a, IRA-400 $FeCl_3Br$	$5.28 \cdot 10^{-6}$	4.3	6.9%
2b, A26 $FeCl_3Br$	$6.06 \cdot 10^{-6}$	4.8	7.2%

*EDS characterization of **2a**, IRA-400 $FeCl_3Br$*

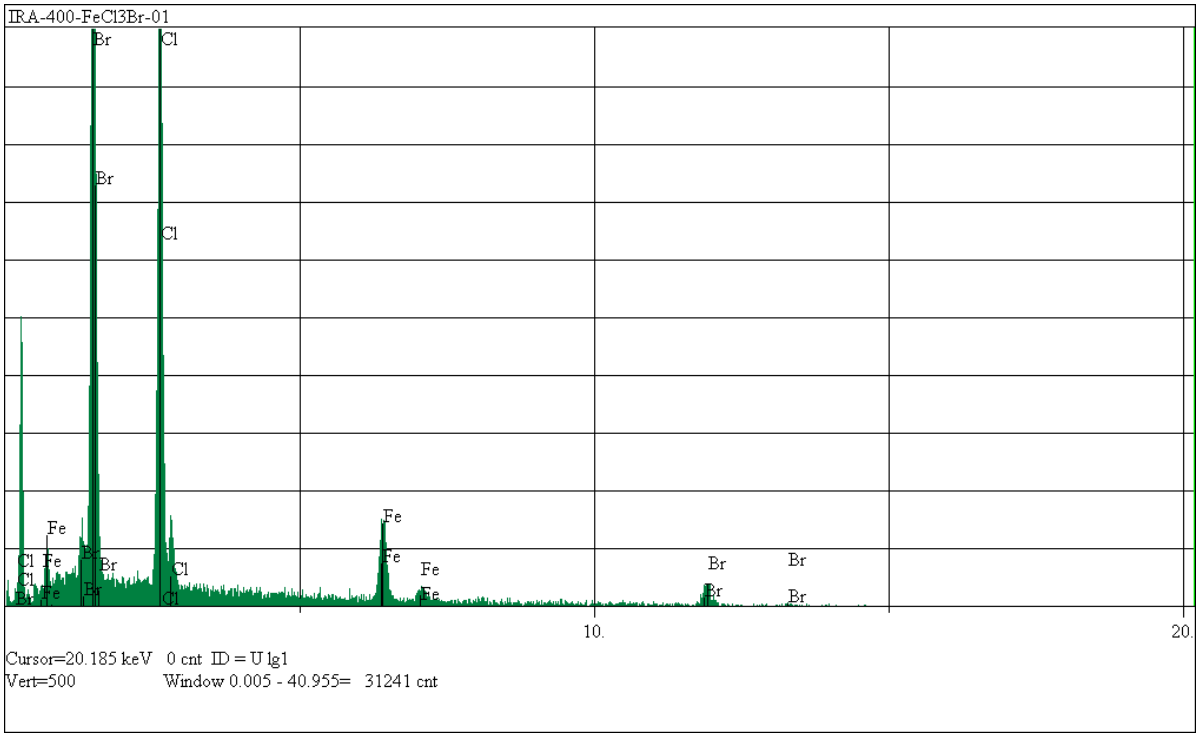

*Figure S 3: EDS spectrum of **2a**, IRA-400 $FeCl_3Br$*

Element	Weight %
Chlorine	37.935
Iron	12.348
Bromine	49.717

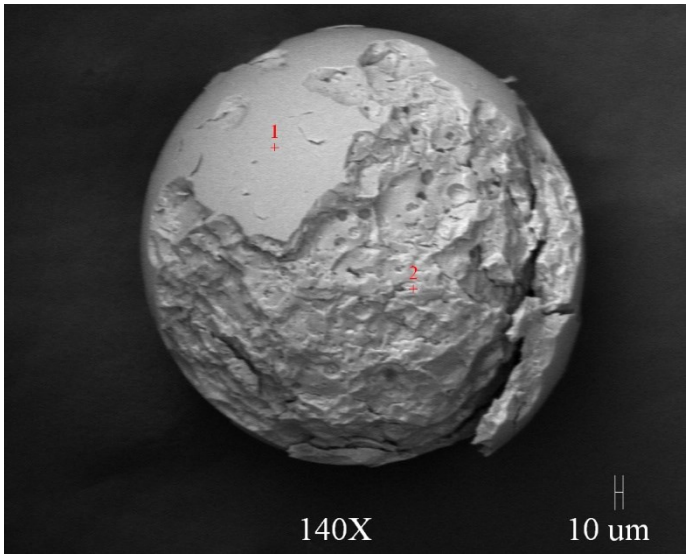

*Figure S 4: SEM image of **2a**, IRA-400 $FeCl_3Br$*

*EDS characterization of **2b**, A26 $FeCl_3Br$*

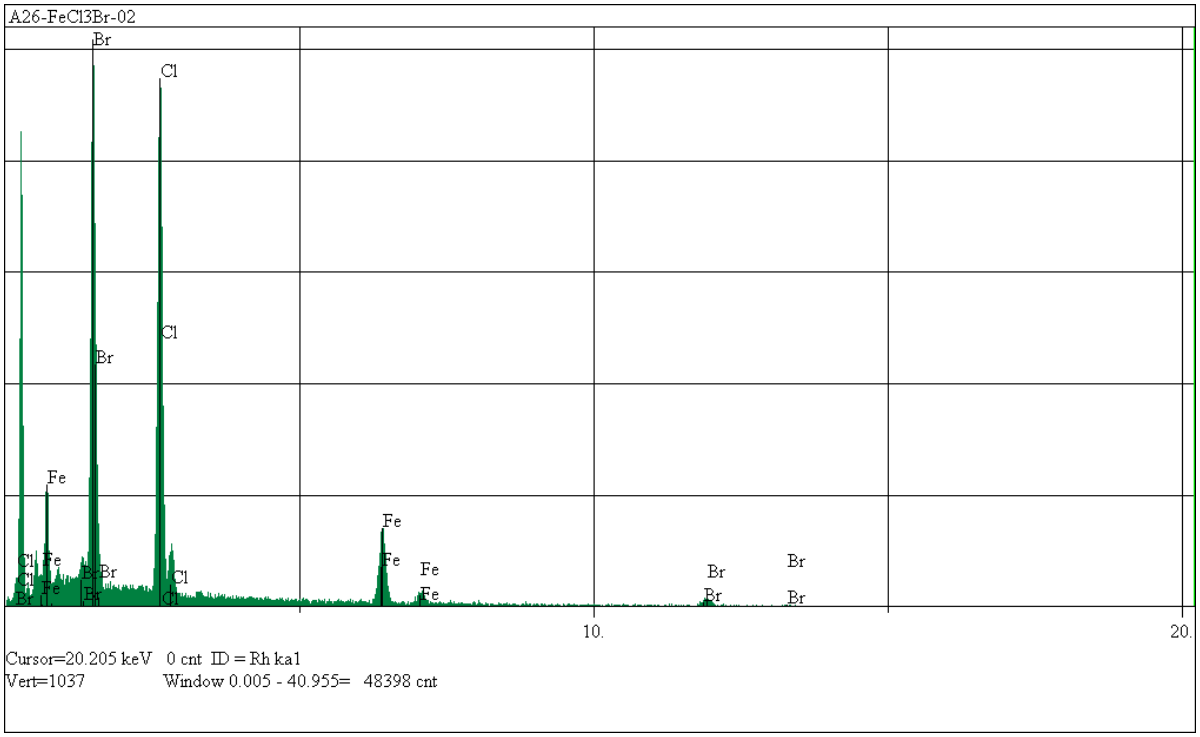

*Figure S 5: EDS spectrum of **2b**, A26 $FeCl_3Br$*

Element	Weight %
Chlorine	40.314
Iron	17.633
Bromine	42.053

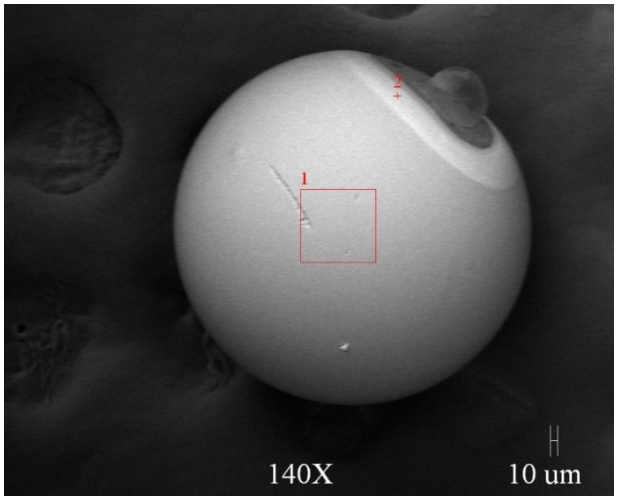

*Figure S 6: SEM image of **2b**, A26 $FeCl_3Br$*

Acquisition conditions

Acquisition time (s) 90.0

Accelerating voltage (kV) 20.0

Metalation with zinc chloride

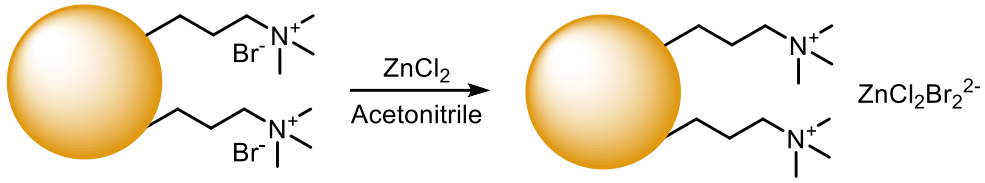

1a, IRA-400 $ZnCl_2Br_2$
1b, A26 $ZnCl_2Br_2$

4 mL of **IRA-400-Br** or **A26-Br** were poured into test tubes containing a 10 mL solution of zinc chloride (anhydrous) in acetone. The necessary zinc chloride mass was calculated based on the maximum theoretical capacity of each resin:

- **IRA-400**: 1.4 meq/mL, which converts into 95.42 mg/mL of zinc chloride (382 mg).
- **A26**: 0.8 meq/mL, which converts into 54.53 mg/mL of zinc chloride (218 mg).

The tubes were then placed onto a vibromechanical agitator overnight. The resins were filtered and washed 5 times with 10 mL of acetone and 3 times with 10 mL of dichloromethane. To avoid pores' collapse, the resins were not dried under vacuum. The products were then analyzed with SEM-EDS spectroscopy to evaluate correct metalation (Figure S 7 and Figure S 9).

*EDS characterization of **1a**, IRA-400 $ZnCl_2Br_2$*

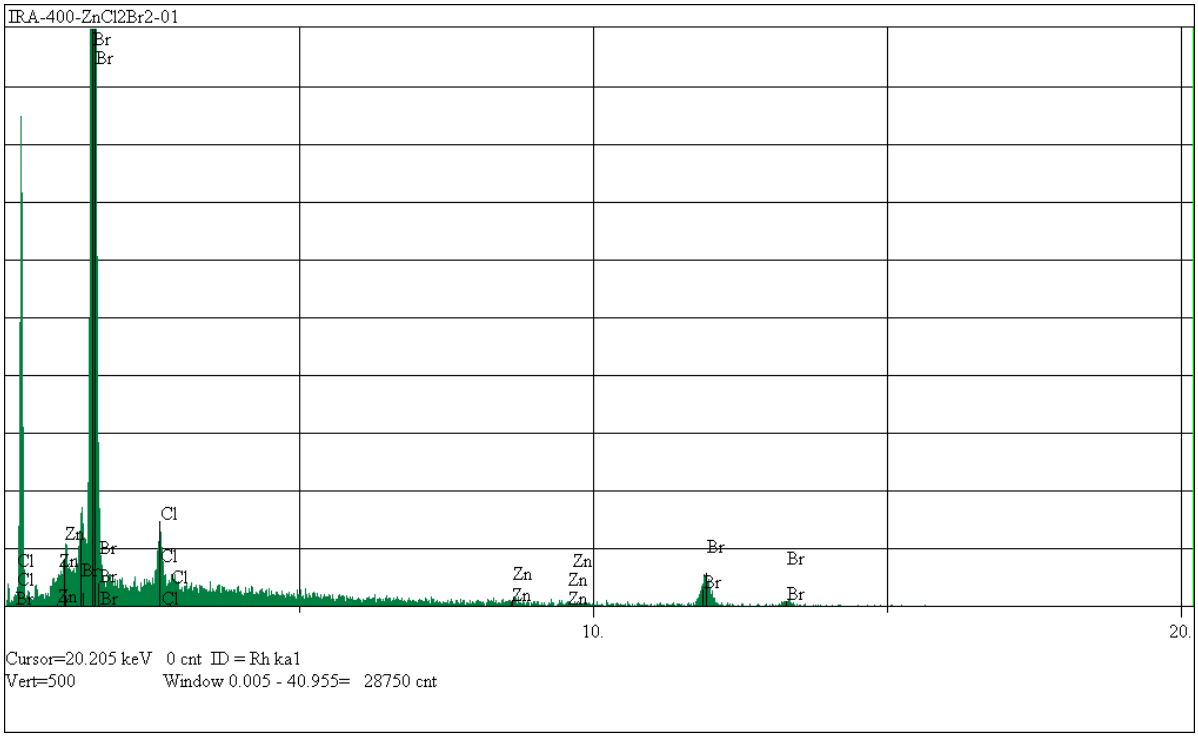

*Figure S 7: EDS spectrum of **1a**, IRA-400 $ZnCl_2Br_2$*

Element	Weight %
Chlorine	5.071
Zinc	1.720
Bromine	93.209

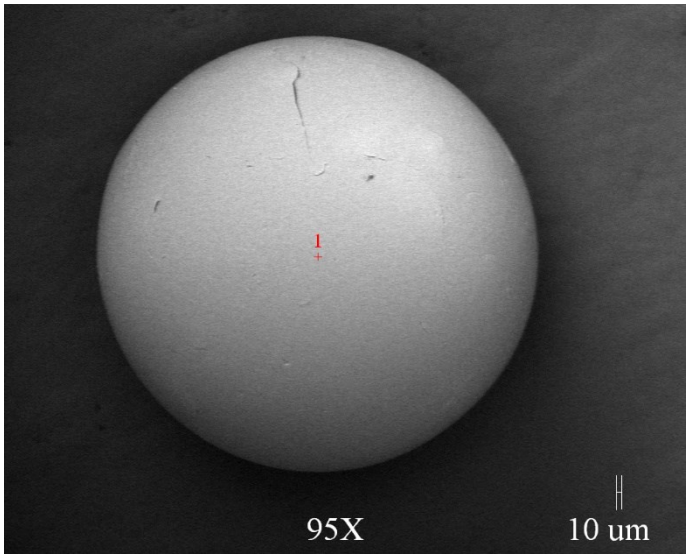

*Figure S 8: SEM image of **1a**, IRA-400 $ZnCl_2Br_2$*

*EDS characterization of **1b**, A26 $ZnCl_2Br_2$*

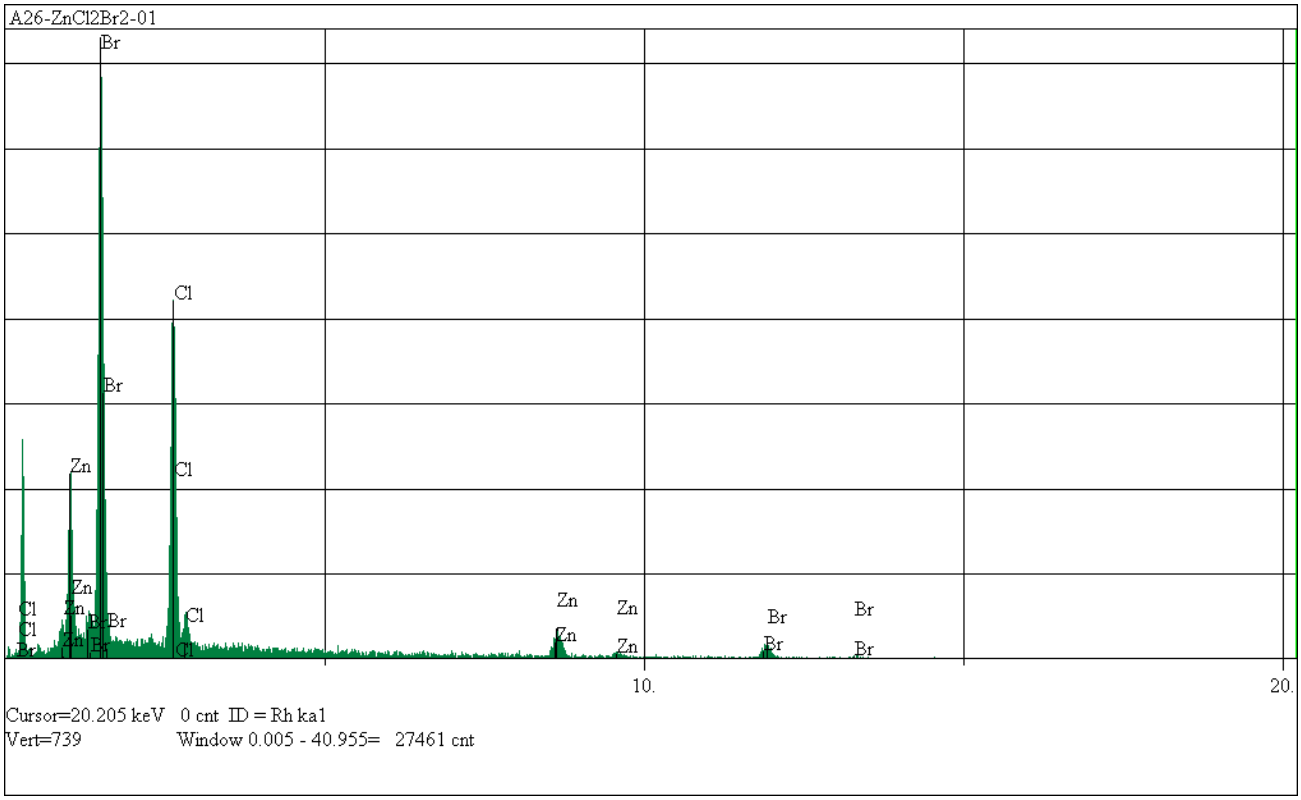

*Figure S 9: EDS spectrum of **1b**, A26 $ZnCl_2Br_2$*

Element	Weight %
Chlorine	31.223
Zinc	13.958
Bromine	54.820

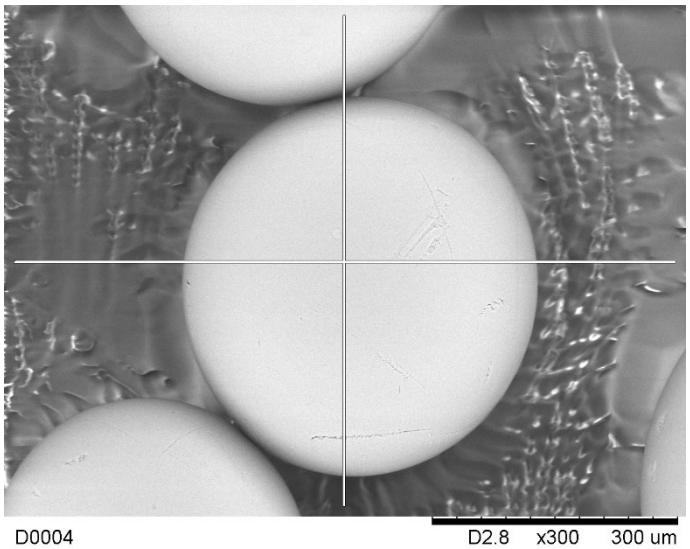

*Figure S 10: SEM image of **1b**, A26 $ZnCl_2Br_2$*

Raman spectra of the resins

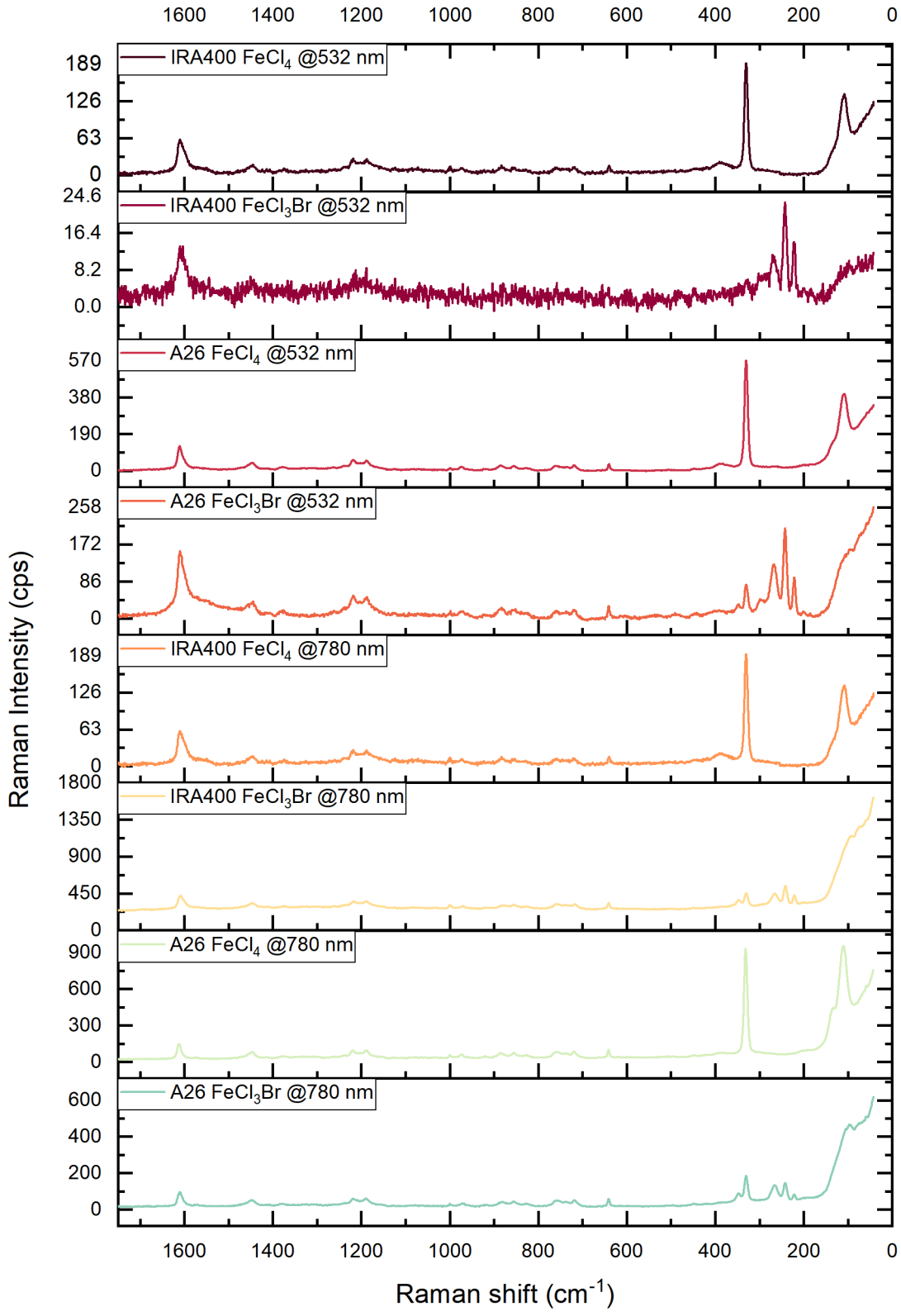

*Figure S 11: Raman spectra of iron-functionalized resins **2a** and **2b**, compared with **IRA400 FeCl$_4$** and **A26 FeCl$_4$** synthetized directly by mixing commercial **IRA400-Cl** and **A26-Cl** resin with iron(III) chloride*

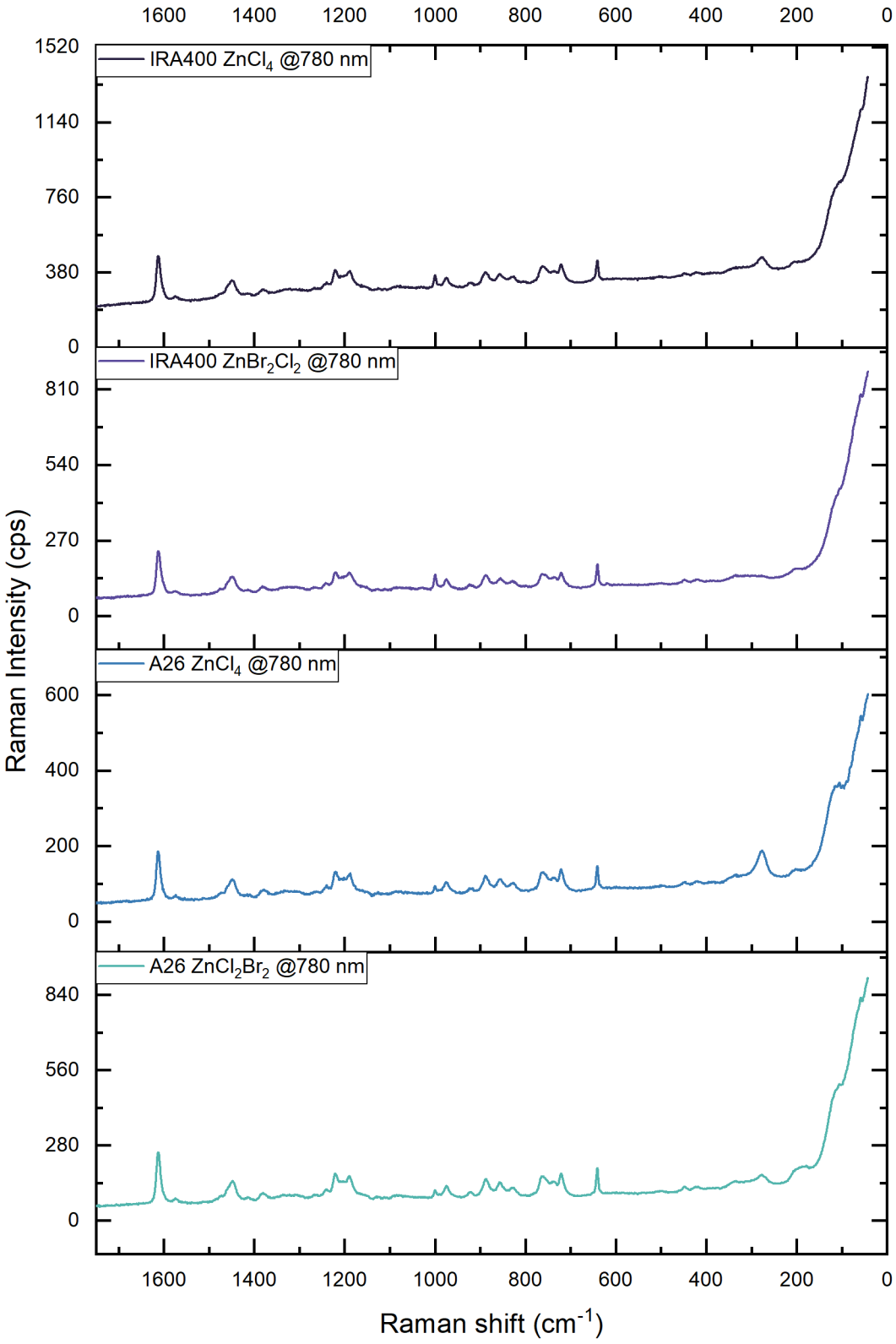

*Figure S 12: Raman spectra of zinc functionalized resins **1a** and **1b**, compared with **IRA400 ZnCl4** and **A26 ZnCl4** synthetized directly by mixing commercial **IRA400-Cl** and **A26-Cl** resin with zinc(II) chloride*

Optimization of the reaction

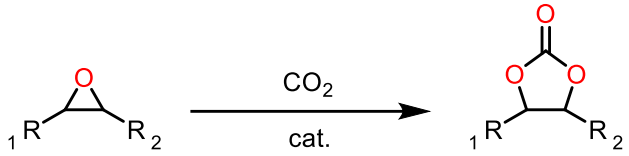

General catalytic procedure. The catalyst (1-30 mg/mmol) and the epoxide (500 mg) were mixed together in an oven-dried autoclave vial. The vial was equipped with a magnetic stirring bar, sealed with an adequate cap, and secured in a stainless steel 300 mL Parr autoclave reactor. The autoclave was then loaded with CO_2 at the desired pressure (0.2-2 MPa) and placed in a pre-heated bath at 50-100°C for the desired reaction time (0.5-16 hours). The autoclave was then cooled at 0°C to quench the reaction and slowly vented off. The reaction mixture was either dissolved in an appropriate solvent and filtered to remove the resin or directly filtered when the product was in the liquid form. Yield was calculated with GC analysis or ^{1}H-NMR using an appropriate internal standard. Isolated products were purified either by precipitation with hexanes or by flash chromatographic column (silica gel, 60 µm, *n*-hexane/ethyl acetate solutions were used as eluent in various proportions).

Experimental design.

To efficiently probe the entirety of the experimental space, experimental design was employed. Because of the large number of experimental variables (catalyst type, catalytic loading, reaction time, substrate, pressure, temperature), the optimization experiment was divided in two parts: the first one (*the screening*) was performed to reduce either the number of variables, excluding the insignificant ones, or to reduce the number of *levels* in the discreet variables, for example determining which catalysts or substrates are poorly performing in the whole experimental space. The second part (*the optimization*) was performed to find the optimal conditions of the reactions using the reduced experimental space, and to build a statistical model that could reliably describe the reactivity of the system at the various conditions. By adopting this approach, the exploration of the entire experimental space is ensured. Moreover, the model can produce many optimized conditions, according to the specific requirements of the user (i.e., low pressures can be prioritized as the first requirement, and the system can be thus optimized with these restrictions. The same can be done for low temperatures, catalyst loading, etc., obtaining from the model many optimized conditions tailored to the requirements of the user).

Screening

The screening was performed at a CO_2 pressure of 10 atmospheres and a temperature of 100°C, to study the effect of the following variables, using a factorial method (split-plot D-optimal design):

- Resins: **1a**, IRA-400 $ZnCl_2Br_2$, **1b**, A26 $ZnCl_2Br_2$, **2a**, IRA-400$FeCl_3Br$, **2b**, A26 $FeCl_3Br$
- Catalyst loading: 1 mg/mmol-20 mg/mmol
- Time: 1 h-16 h
- Substrates: cyclohexene oxide, styrene oxide, propylene oxide

As all the experiments were carried out in a single steel autoclave, simultaneous runs had to be performed with some restrictions. Thus, we decided to adopt a split-plot design, which accounts for *hard to change* (HTC) factors, such as the duration of the experiment. Therefore, experiments were grouped in batches, inside which this factor was kept constant, and the other variables (resin type, catalyst loading and substrate) were changed. Since the main goal of the screening experiment was to determine which factors were relevant to the yield of the reaction, CO_2 pressure and temperature were set respectively at 1 MPa and 100°C for the entire duration of the screening, as we knew from previous knowledge that they were highly influential on the yield of the reaction. As for the screening, we chose a factorial design. The full-factorial design would need, if randomized, a total of 48 runs ($4^1 \cdot 3^1 \cdot 2^2$). Thus, we decided to fractionate the design, using D-optimality as the statistic criterion, obtaining 34 runs grouped in 8 batches. Even though conversion was measured for styrene and cyclohexene oxide, only yield was analyzed as the response. Here the data from the screening is reported.

Table S 3: Screening results. Conditions: p = 1.0 MPa, T = 100°C. Yield determined with GC-FAST analysis, using dodecane as IS.

Group	Run	Time (h)	Catalyst	Catalyst loading (mg/mmol)	Substrate	Yield (%)
1	1	16	IRA 400$ZnCl_2Br_2$	1	Propylene oxide	37.2
1	2	16	A26 $ZnCl_2Br_2$	1	Cyclohexene oxide	0
1	3	16	A26 $FeCl_3Br$	20	Propylene oxide	88.9
1	4	16	IRA 400$ZnCl_2Br_2$	1	Styrene oxide	0
2	5	1	A26 $FeCl_3Br$	1	Styrene oxide	0
2	6	1	IRA 400$ZnCl_2Br_2$	1	Propylene oxide	1.6
2	7	1	IRA 400$FeCl_3Br$	1	Cyclohexene oxide	0
2	8	1	A26 $ZnCl_2Br_2$	20	Styrene oxide	57.3
3	9	1	A26 $ZnCl_2Br_2$	20	Propylene oxide	100
3	10	1	A26 $ZnCl_2Br_2$	1	Styrene oxide	5.4
3	11	1	A26 $ZnCl_2Br_2$	1	Cyclohexene oxide	0
3	12	1	IRA400 $FeCl_3Br$	1	Propylene oxide	2.7
3	13	1	A26 $FeCl_3Br$	20	Styrene oxide	23.9
4	14	16	IRA400 $FeCl_3Br$	20	Propylene oxide	11.1
4	15	16	A26 $FeCl_3Br$	20	Cyclohexene oxide	22.9
4	16	16	A26 $FeCl_3Br$	1	Propylene oxide	29.2
4	17	16	A26 $ZnCl_2Br_2$	20	Styrene oxide	100
5	18	1	A26 $ZnCl_2Br_2$	20	Cyclohexene oxide	0
5	19	1	IRA 400$ZnCl_2Br_2$	20	Propylene oxide	23.2
5	20	1	A26 $ZnCl_2Br_2$	1	Propylene oxide	7.1
5	21	1	A26 $FeCl_3Br$	1	Cyclohexene oxide	0
6	22	16	IRA400 $FeCl_3Br$	20	Cyclohexene oxide	0
6	23	16	A26 $FeCl_3Br$	20	Styrene oxide	79
6	24	16	IRA400 $ZnCl_2Br_2$	20	Propylene oxide	90.2
6	25	16	IRA400 $FeCl_3Br$	1	Propylene oxide	9.1
7	26	16	IRA400 $ZnCl_2Br_2$	1	Cyclohexene oxide	0
7	27	16	IRA400 $FeCl_3Br$	1	Styrene oxide	2.6
7	28	16	IRA400 $ZnCl_2Br_2$	20	Styrene oxide	73.4
7	29	16	A26 $FeCl_3Br$	1	Styrene oxide	17.8
7	30	16	A26 $ZnCl_2Br_2$	1	Propylene oxide	76.8
8	31	1	IRA400 $ZnCl_2Br_2$	1	Styrene oxide	2.98
8	32	1	IRA400 $FeCl_3Br$	20	Styrene oxide	3.08
8	33	1	IRA400 $ZnCl_2Br_2$	20	Cyclohexene oxide	0
8	34	1	A26 $FeCl_3Br$	20	Propylene oxide	87

Methodology:

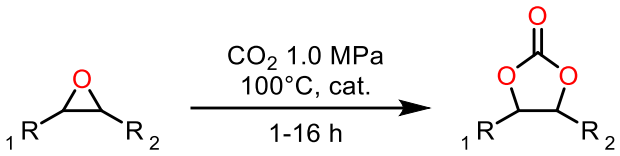

Propylene oxide (R_1 = Me, R_2 = H)

The catalyst (loading = 1-20 mg/mmol) and propylene oxide (500 mg, 8.6 mmol) were added in an autoclave vial capped with a septum. The vial was transferred to a Parr steel autoclave, which was loaded with 1.0 MPa of CO_2 and heated at 100°C. After a reaction time of 1-16 hours, the autoclave was cooled at 0°C. The reaction mixture was diluted with ethyl acetate and filtered to remove the resin. Yield was calculated via fast GC-FID analysis.

Styrene oxide (R_1 = Ph, R_2 = H)

The catalyst (loading = 1-20 mg/mmol) and styrene oxide (500 mg, 4.16 mmol) were added in an autoclave vial capped with a septum. The vial was transferred to a Parr steel autoclave, which was loaded with 1.0 MPa of CO_2 and heated at 100°C. After 1-16 hours the autoclave was cooled at 0°C. When the reaction didn't proceed to completion, the carbonate was solubilized in epoxide, and the procedure for yield determination was the same as for propylene oxide. When the epoxide was completely converted to styrene carbonate, conversely, the solid product needed to be dissolved in dichloromethane. The resin was then removed by filtration and the solvent was evaporated under reduced pressure. Yield was calculated by fast GC-FID analysis.

Cyclohexene oxide (R_1 = R_2 = Cy)

The catalyst (loading = 1-20 mg/mmol) and cyclohexene oxide (500 mg, 8.6 mmol) were added in an autoclave vial capped with a septum. The vial was transferred to a Parr steel autoclave, which was loaded with 1.0 MPa of CO_2 and heated at 100°C. After 1-16 hours, the autoclave was cooled at 0°C. The reaction mixture is diluted with ethyl acetate and filtered to remove the resin. Yield was calculated by fast GC-FID analysis.

Design of experiment – model selection

To reduce the non-normality of the errors in the linear model, and often to improve linearity itself, a power transform can be applied to the model. In a linear model:

$$Y_i = \beta_0 + \beta \mathbf{X} + \varepsilon_i, \quad \varepsilon_i \sim \mathcal{N}(0, \sigma^2)$$

Where Y_i is the response variable (in our case, the yield), β_0 is the intercept, β are the coefficients for the variables $\mathbf{X}$, and ε_i are the errors, which follow a normal distribution centered around 0, the simple Box-Cox transform is:

$$Y_i^{(\lambda)} = \begin{cases} \dfrac{Y_i^{\lambda} - 1}{\lambda} & for\ (\lambda \neq 0) \\ \log(Y_i) & for\ (\lambda = 0) \end{cases}$$

The λ parameter is determined by maximum likelihood, i.e., which value of λ is most likely to have given rise to the observed distribution of the model residuals. When plotting the negative double logarithm of the likelihood function $\mathcal{L}$ for $\lambda = [-3 \ldots 3]$ (Figure S 13), the minimum of the function can be assumed to be the correct λ value. In this case, the minimum was near $\lambda = 0.5$, which corresponds to a square root transform. Because the response needs to be greater than zero, an arbitrary constant was added. Thus the transform applied to the data is:

$$Y_i^{(\lambda)} = \sqrt{Y_i + 0.1}$$

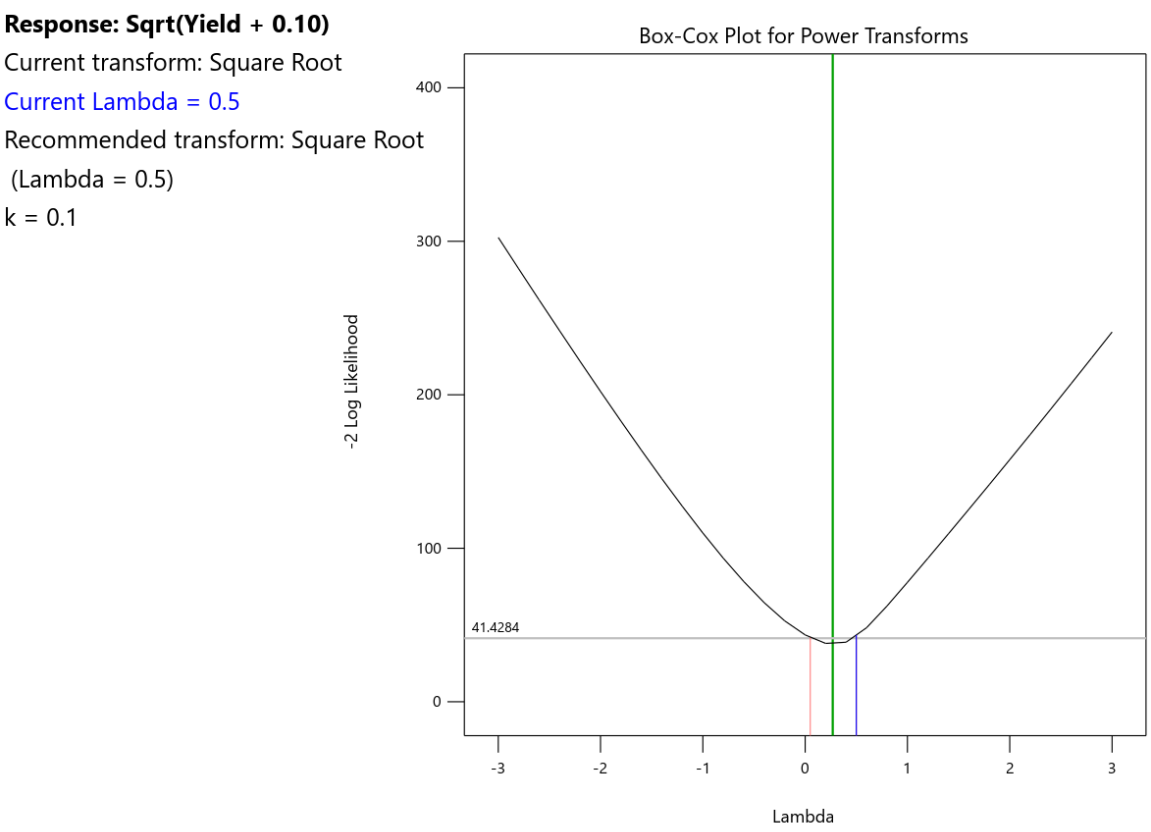

Figure S 13: Box-Cox plot of the screening experiment

The model parameters were chosen with a simple algorithm that removed terms with p-values greater than 0.1, starting from the two-factor interaction model and running backwards. As a result, these parameters were chosen (Table S 4).

Table S 4: Model parameters statistics

Source	Term degrees of freedom	F-value	p-value	
Whole-plot	1	6.51	0.0566	not significant
a – Time	1	6.51	0.0566	
Subplot	17	24.27	< 0.0001	significant
B – Resin	3	25.59	< 0.0001	
C - Catalyst loading	1	48.33	< 0.0001	
D - Substrate	2	64.49	< 0.0001	
BC	3	7.36	0.0088	
BD	6	4.88	0.0167	
CD	2	10.74	0.0048	

Although time as a parameter did not result significant, it was close to the threshold p-value of significance (0.05). Thus, it was still considered for the optimization. All the other variables, on the other hand, were significant and considered for the model. The regression results are here reported (Table S 5), along with a bar graph to visualize the coefficients (Figure S 14).

Table S 5: Coefficient estimate. Factors are coded, meaning levels are coded as -1/+1 and not as experimental values.

Source	Coefficient Estimate	Standard Error
Intercept	3.56	0.4857
Whole-plot Terms:		
a-**Time**	1.24	0.4866
Subplot Terms:		
B[1]-**Resin**	1.93	0.3324
B[2]	1.37	0.3098
B[3]	-0.8215	0.3456
C-**Catalytic loading**	1.39	0.2001
D[1]-**Substrate**	2.38	0.2419
D[2]	-0.0168	0.2701
B[1]C	0.8965	0.3147
B[2]C	0.1986	0.3203
B[3]C	0.4274	0.3091
B[1]D[1]	0.5965	0.4599
B[2]D[1]	-0.5184	0.4923
B[3]D[1]	1.01	0.486
B[1]D[2]	0.806	0.4757
B[2]D[2]	-0.5131	0.4821
B[3]D[2]	0.5253	0.4159
CD[1]	0.2159	0.2386
CD[2]	0.8904	0.2361

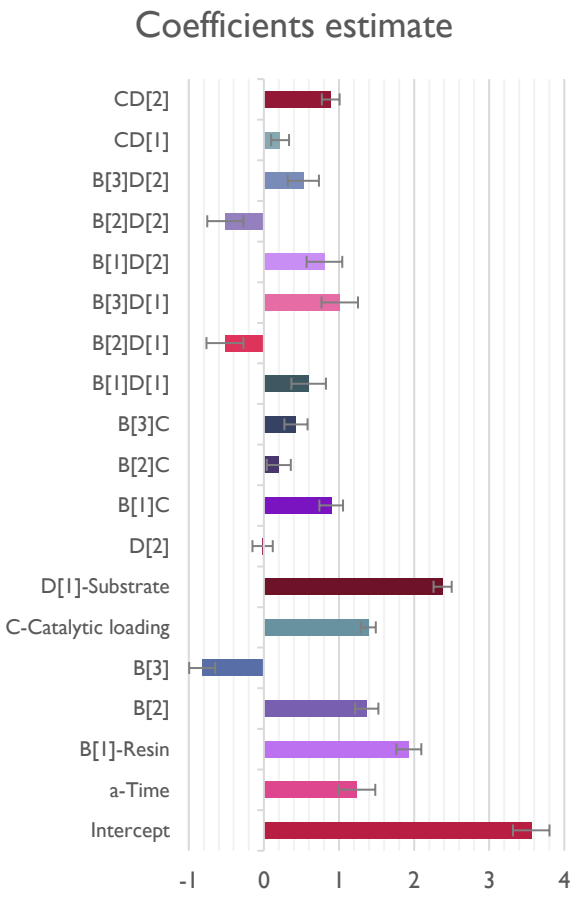

Figure S 14: Coefficients estimate: graphical depiction

The screening allowed us to identify the **A26** resins as best performing compared to the **IRA-400** resins. Moreover, as displayed in Figure S 15, zinc catalysts performed consistently better than their ferric equivalents. However, because of iron's high availability and its promising results when combined with the **A26** resin, we decided to further study its catalytic activity in the next step of the optimization. In addition, both time and catalyst loading were found to be highly influential in this reaction. Especially a higher catalyst loading was needed to obtain desirable results, and when it was lowered to 1 mg/mL the yield was found to be seriously compromised.

The model is not significant for cyclohexene oxide since it proved to be quite unreactive with all the catalysts we used, and almost all the tests we ran did not yield the desired product at all.

We therefore decided to further optimize the reaction on propylene oxide and styrene oxide, using the resins **A26 $FeCl_3Br$** and **A26 $ZnCl_2Br_2$** as catalysts.

Factor Coding: Actual
Response: Yield (%)

Actual Factors:
a: Time = Average over
C: Catalyst loading = Average over

D1 Propylene oxide
D2 Styrene Oxide
D3 Cyclohexene oxide

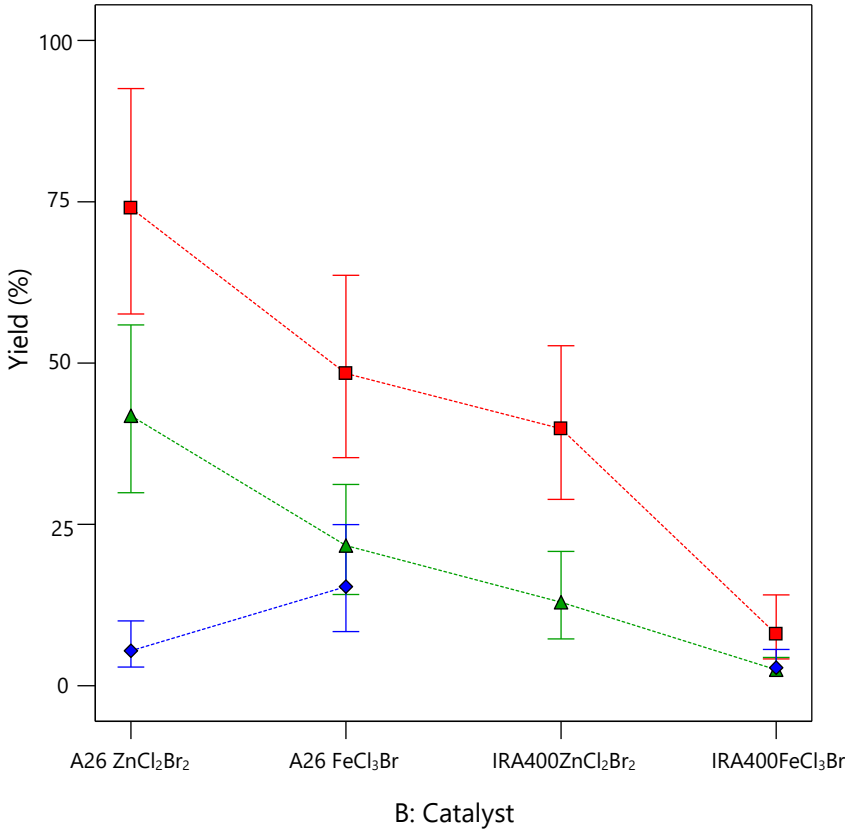

Figure S 15: Interaction between catalyst choice and substrate. Some results are truncated due to a transform error (Yield < 0)

Optimization

The optimization experiment aims is to find the most desirable reaction conditions. To do this, a detailed model of the reactivity is studied in a pre-defined experimental space, probing all the relevant variables, and then it's optimized to find the most suitable conditions. In this way, for example, yield can be maximized, while minimizing some factors like temperature, pressure and reaction time, thus obtaining more efficient conditions. Moreover, using design of experiment, the risk of probing only a minor part of the experimental space is avoided, and using response surface methods, the non-linearity of the response of the system is taken into account. Therefore, in this phase we decided to study the following variables, using a response surface method (split-plot I-optimal design, hard-to-change factors are denoted as "HTC"), and planning to build a quadratic model:

- Pressure: 0.2-2 MPa (htc)
- Temperature: 50-100°C (htc)
- Time: 0.5-16 h (htc)
- Resins: **2b**, A26 $FeCl_3Br$, **1b**, A26 $ZnCl_2Br_2$
- Catalyst Loading: 5-30 mg/mmol
- Substrates: propylene oxide, styrene oxide

The experimental procedures are the same as for the screening experiment. Next are reported the data of the obtained by the optimization experiment.

Table S 6: Optimization results. Yield determined with GC-FAST analysis, using dodecane as IS.

Group	Run	a: Pressure (MPa)	b: Temperature (°C)	c: Time (h)	D: Catalyst loading (mg/mmol)	E:Substrate	F:Resin	Yield (%)
1	1	1.1	50	16	26	Styrene oxide	A26 $FeCl_3Br$	32.2
1	2	1.1	50	16	5	Propylene oxide	A26 $ZnCl_2Br_2$	40.4
2	3	1	100	13	22	Propylene oxide	A26 $ZnCl_2Br_2$	99.8
2	4	1	100	13	5	Styrene oxide	A26 $FeCl_3Br$	61.8
3	5	1.4	76	7.79	30	Propylene oxide	A26 $FeCl_3Br$	75.2
3	**6[a]**	**1.4**	**76**	**7.79**	**20**	**Styrene oxide**	**A26 $ZnCl_2Br_2$**	**24.7**
4	7	2	50	0.5	8	Styrene oxide	A26 $ZnCl_2Br_2$	0
4	8	2	50	0.5	30	Propylene oxide	A26 $ZnCl_2Br_2$	7
4	9	2	50	0.5	5	Propylene oxide	A26 $FeCl_3Br$	3.7
5	10	2	100	16	5	Styrene oxide	A26 $ZnCl_2Br_2$	93.5
5	11	2	100	16	15	Propylene oxide	A26 $FeCl_3Br$	92.2
5	12	2	100	16	30	Styrene oxide	A26 $FeCl_3Br$	99
6	13	2	63	14	28	Propylene oxide	A26 $ZnCl_2Br_2$	41.2
6	14	2	63	14	8	Styrene oxide	A26 $FeCl_3Br$	25.8
7	15	1.2	76	6.78	13	Propylene oxide	A26 $ZnCl_2Br_2$	95
7	16	1.2	76	6.78	11	Propylene oxide	A26 $FeCl_3Br$	90.6
8	17	0.2	76	16	11	Styrene oxide	A26 $FeCl_3Br$	24.6
8	18	0.2	76	16	6	Propylene oxide	A26 $FeCl_3Br$	0
8	19	0.2	76	16	30	Propylene oxide	A26 $ZnCl_2Br_2$	0
9	20	0.2	50	7.24	5	Styrene oxide	A26 $FeCl_3Br$	5.7
9	21	0.2	50	7.24	30	Styrene oxide	A26 $ZnCl_2Br_2$	18.4
9	22	0.2	50	7.24	22	Propylene oxide	A26 $FeCl_3Br$	4.4
10	23	0.6	68	0.5	20	Propylene oxide	A26 $ZnCl_2Br_2$	9.1
10	24	0.6	68	0.5	30	Styrene oxide	A26 $FeCl_3Br$	6.35
11	25	0.2	100	0.5	5	Styrene oxide	A26 $ZnCl_2Br_2$	0
11	26	0.2	100	0.5	6	Propylene oxide	A26 $FeCl_3Br$	0
12	27	2	100	0.5	30	Styrene oxide	A26 $ZnCl_2Br_2$	51.7
12	28	2	100	0.5	17	Styrene oxide	A26 $FeCl_3Br$	18.4
12	29	2	100	0.5	5	Propylene oxide	A26 $ZnCl_2Br_2$	20.1
13	30	0.2	100	9.03	5	Propylene oxide	A26 $ZnCl_2Br_2$	0
13	31	0.2	100	9.03	24	Styrene oxide	A26 $FeCl_3Br$	12.9
13	32	0.2	100	9.03	30	Propylene oxide	A26 $FeCl_3Br$	1
14	33[b]	2	50	0.5	8	Styrene oxide	A26 $ZnCl_2Br_2$	1.2
15	34[c]	1.4	76	7.79	20	Styrene oxide	A26 $ZnCl_2Br_2$	92.7
15	35[b]	1.4	76	7.79	30	Propylene oxide	A26 $FeCl_3Br$	85.3
16	36[d]	0.2	76	16	11	Styrene oxide	A26 $ZnCl_2Br_2$	32.6

[a]Run 6 was found to be an outlier and thus was repeated. [b]Run 33 and 35 are repetitions of run 7 and run 5, respectively. They were repeated to improve statistics, as these points were found to have high leverage (>1). [c]Run 34 is the repetition of run 6. [d]Run 36 was

added because run 17 should have been done with catalyst **1b**, A26 $ZnCl_2Br_2$, but it was erroneously performed with **2b**, A26 $FeCl_3Br$.

Notes:

- The reactions conducted under a CO_2 pressure of 2 bars with propylene oxide afforded a 0% yield since propylene oxide at this pressure boils at 34°C before it has a chance to react.
- The A26 $FeCl_3Br$ resin probably leaches Fe salts and/or degrades in harsher reaction conditions (unknown peaks in the chromatogram); this can sometimes lead to overestimating yield.

Design of experiment – model selection

Like the screening experiment, the optimization needed a data transformation. In this case, a square root transform was again the most suitable, using an arbitrary constant equal to 0.0998. However, because the prediction of high yield values was too overestimated by this method, we decided to keep the data with no transform.

The selection of the model terms instead was performed with the same algorithm as the screening experiment, although no parameter was needed to be added to maintain proper hierarchy. These parameters were chosen (Table S 7).

Table S 7: optimization model parameters

Source	Term degrees of freedom	F-value	p-value
Whole-plot	4	10.92	0.0008
a-Pressure	1	10.88	0.004
b-Temperature	1	10.81	0.0097
c-Time	1	10.89	0.0379
a^2	1	11.04	0.0018
Subplot	14	5.31	0.0055
D-Catalyst loading	1	5.35	0.0012
E-Substrate	1	5.37	0.041
F-Resin	1	5.37	0.0004
aD	1	5.81	0.0062
aE	1	5.46	0.0014
bD	1	5.3	0.0007
bE	1	5.28	0.055
cD	1	5.47	0.0176
cE	1	5.69	0.0015
cF	1	5.64	0.01
DE	1	5.43	0.0366
DF	1	5.72	0.0394
EF	1	6.15	0.0069
D^2	1	5.35	0.0036

Next, the regression results are here reported (Table S 8), along with a bar graph to visualize the coefficients (Figure S 16).

Table S 8: Coefficients estimate. Factors are coded, meaning levels are coded as -1/+1 and not as experimental values.

Source	Coefficient Estimate	Standard Error
Intercept	72.36	8.57
Whole-plot Terms:		
a-**Pressure**	21.62	5.96
b-**Temperature**	19.64	6.26
c-**Time**	14.45	6.12
a^2	-43.94	10.75
Subplot Terms:		
D-**Catalytic loading**	6.08	0.9755
E-**Substrate**	2.12	0.7911
F-**Resin**	6.21	0.7784
aD	5.95	1.42
aE	-5.48	0.9182
bD	8.45	1.22
bE	-2.38	0.9687
cD	-4.84	1.44
cE	6.71	1.18
cF	4.36	1.15
DE	2.9	1.05
DF	-3.72	1.4
EF	5.04	1.27
D^2	-9.79	1.99

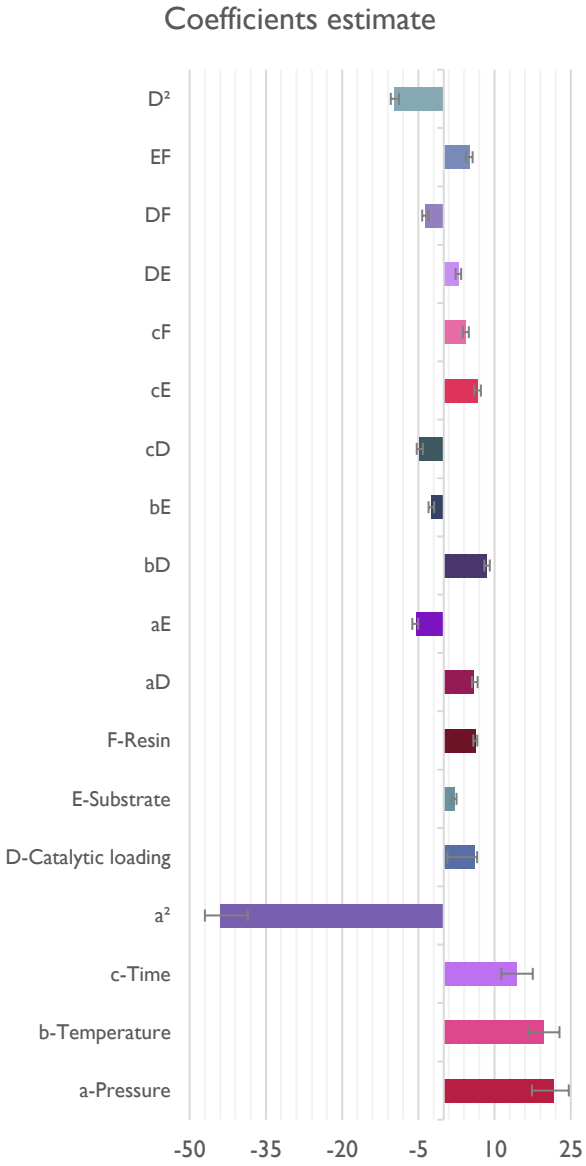

Figure S 16: Bar graph of the coded coefficients. The intercept was excluded for readability

The most impactful term of the model is clearly pressure, along with its square term. Indeed, when going from lower pressures (0.2-0.4 MPa) to mid pressure (0.8-1.2 MPa), a high initial increase of yield is observed, while higher pressures (> 1.4 MPa) show diminishing returns. Thus, a negative square term was found appropriate to describe this kind of curvature.

This model can describe the reactivity of the system precisely. Furthermore, it can be noticed from the smaller error bars in the coefficients graph how the resolution and precision of the experiment increased. It must be pointed out, however, that such a high negative coefficient for the a^2 term results in underestimated yields in the high-pressure regions (in Figure S 17 it's evident from the green line, i.e. the pressure perturbation plot). Excessively high pressures, however, in fact are not so detrimental to the reaction. Yield thus is slightly overestimated in the 1.1-1.6 MPa region and underestimated over 1.6 MPa. Deviation from experimental data, however, is limited.

Factor Coding: Actual
Response: Yield (%)
Actual Factors:
a: Pressure = 1.1 MPa
b: Temperature = 75 °C
c: Time = 8.25 h
D: Catalytic loading = 17.5 mg/mmol
E: Substrate = Average over
F: Resin = Average over

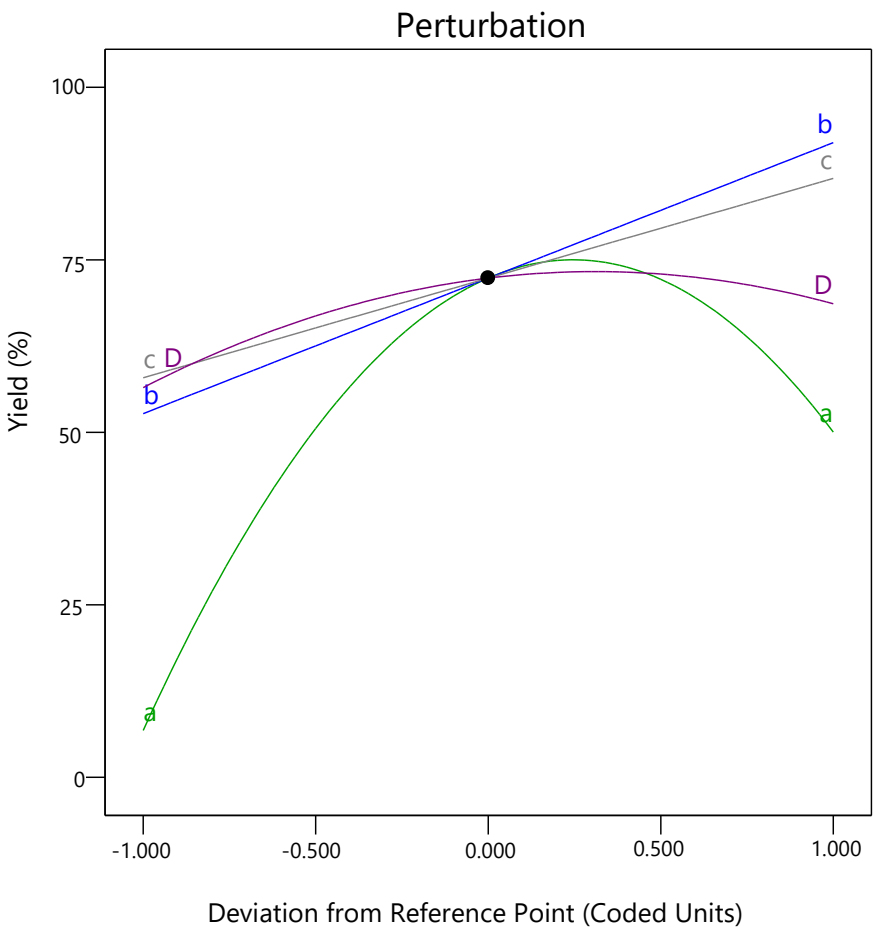

Figure S 17: Perturbation plot. Each line displays how yield changes by perturbing each factor from a center point (in this case, the center of the experimental space).

Design of experiment – conclusions

Pressure. Both styrene oxide and propylene oxide need higher than "mild" pressures to react effectively. This is especially true for propylene oxide (Figure S 18), which reaches the optimal pressure at about 1.4 MPa (when all the other factors are at their center point), while styrene oxide is easily converted at smaller pressures. As already mentioned in the previous paragraph, the activity loss at higher pressures is likely exaggerated by the model, however, with a 0.0018 *p*-value, the a^2 term is significant and vital to correctly model the pressure effects on the system.

Temperature. Temperature increases, up to 100°C, are beneficial for both substrates. Propylene oxide, as for pressure, gains better results than styrene oxide from harsher conditions (Figure S 19).

Time. While with styrene oxide the zinc-based resin is better performing in any reaction time (Figure S 21), with propylene oxide the iron-based resin seems to yield a higher rate in the first part of the reaction, showing better results in short runs, while after long reaction times the zinc-based resin still performs better (Figure S 20). This could be due to different mechanisms, but further inspection is needed to confirm this hypothesis. While the zinc-based resin is superior with styrene oxide, A26 $FeCl_3Br$ could be a compelling solution for propylene oxide and other terminal alkyl epoxides. More generally, styrene oxide requires longer reaction times than propylene oxide.

Catalytic loading. Both substrates benefit from higher catalytic loading, and the decrease in selectivity at higher catalytic loading is limited. In Figure S 22, which is referred to styrene oxide, a local maximum is visible. The same holds true also for propylene oxide. This *morphology* of the regression function identifies a closed area in the experimental space in which the yield can be further optimized.

Optimization. In the optimization step, each factor can be minimized, maximized, or ignored. An importance factor can be introduced to each factor, ranging from 1 to 5 (where 1 is the least important factor and 5 is the most important). Thus, to optimize the reaction, the following criteria were employed:

- Pressure was minimized inside the original range (0.2-2.0 MPa). The importance level is three.
- Temperature was minimized inside the original range (50-100 °C). The importance level is three.
- Reaction time was minimized inside the range 0.5-8 hours. The importance level is three.
- Catalytic loading was minimized inside the original range (5-30 mg/mmol) for styrene oxide and in the 5-20 mg/mmol for propylene oxide. The importance level is three.
- The optimization was repeated for each substrate. Because the zinc-based catalyst was generally better than the iron one, it was chosen for each substrate.
- Yield was maximized over a minimum of 90%. The importance level is 5.

With these parameters in mind, the best results were these:

Substrate	Pressure (MPa)	Temperature (°C)	Time (h)	Catalytic loading (mg/mmol)	Resin	Expected. yield %	Desirability
Propylene oxide	1.35	97.8	6.7	17.5	**1b**, A26 $ZnCl_2Br_2$	93.3	0.091
Styrene oxide	1.23	94.1	6.4	21.7	**1b**, A26 $ZnCl_2Br_2$	97.9	0.170

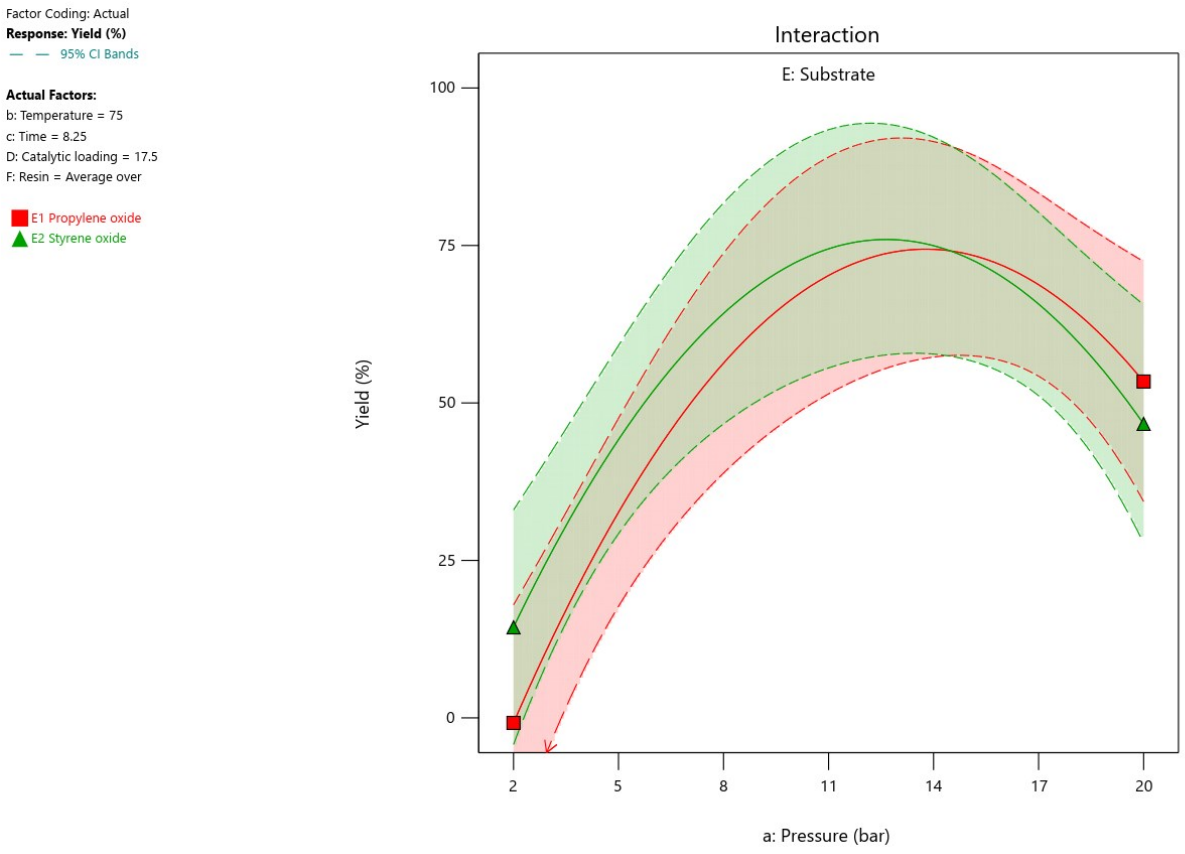

Figure S 18: Interaction between pressure and substrate factors. Other factors are at their center point, and catalyst effects are averaged

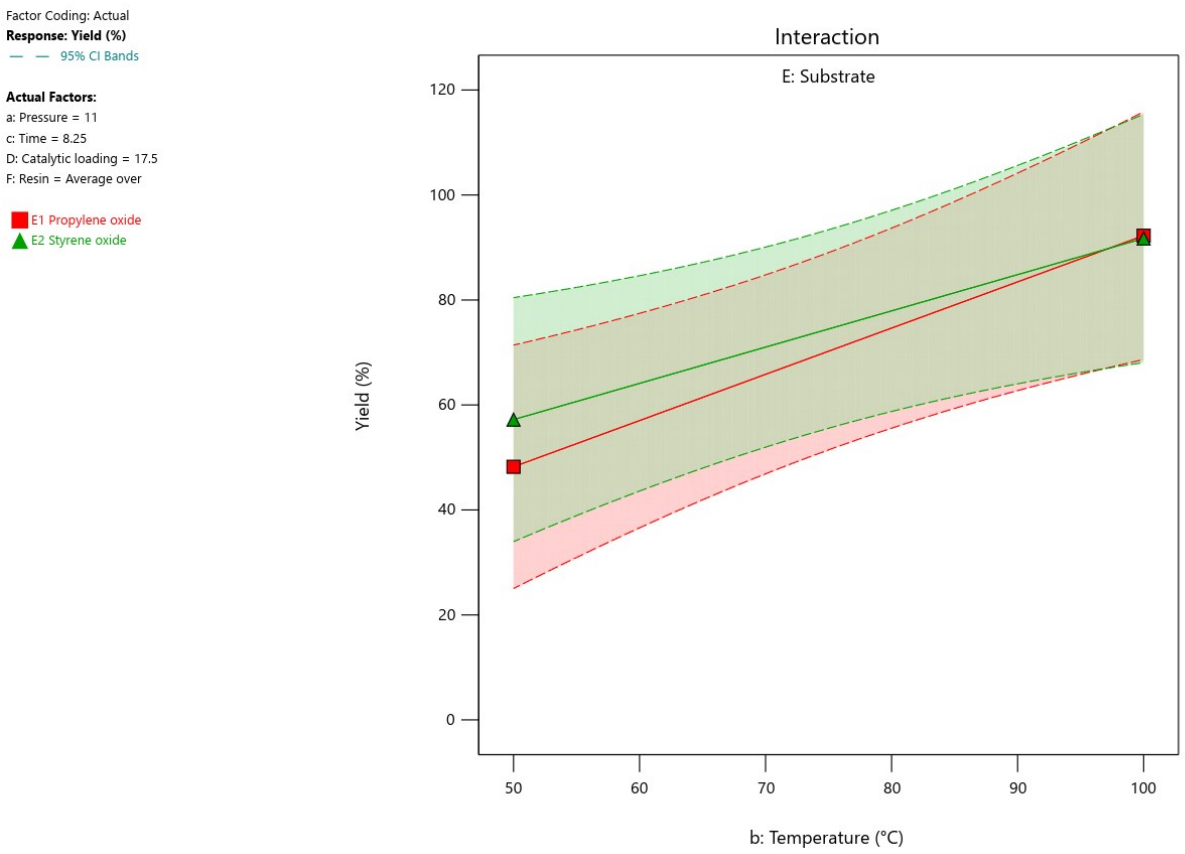

Figure S 19: interaction between temperature and substrate factors. Other factors are at their center point, and catalyst effects are averaged

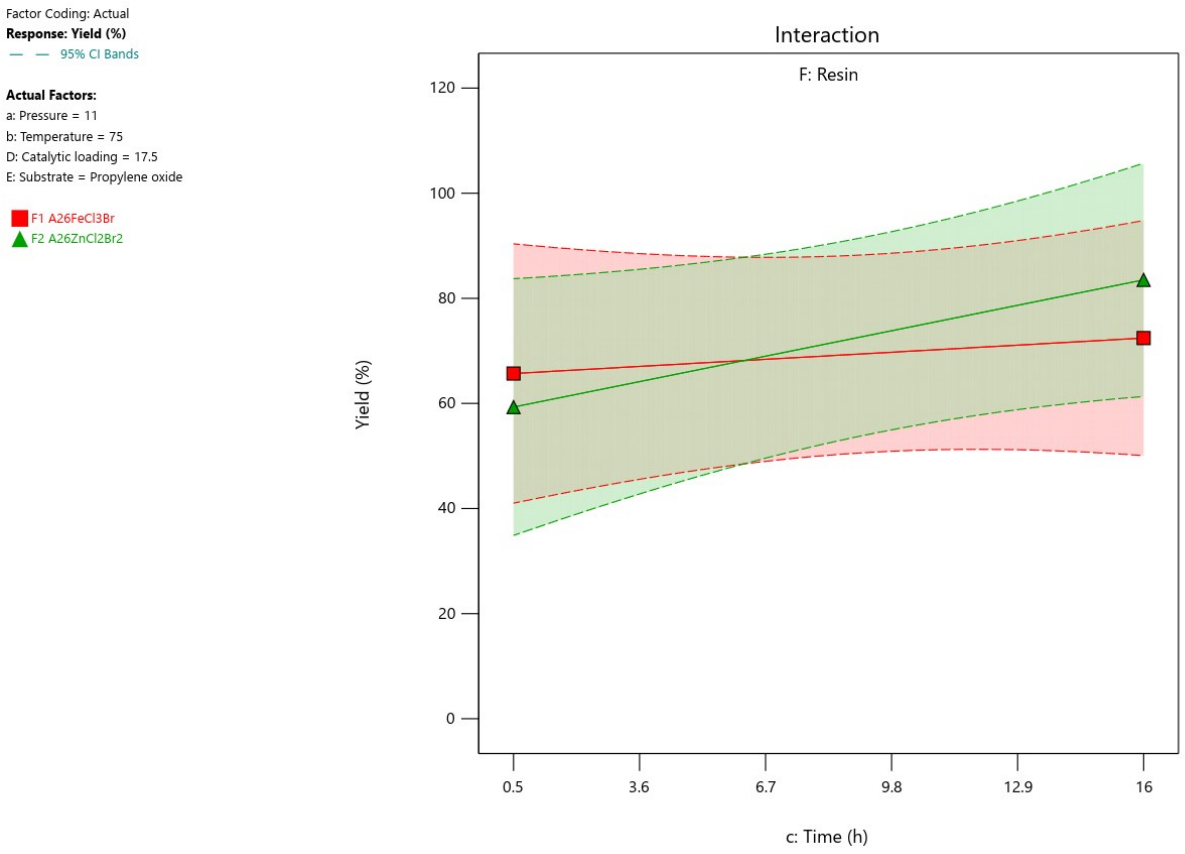

Figure S 20: interaction between reaction time and catalyst type for propylene oxide

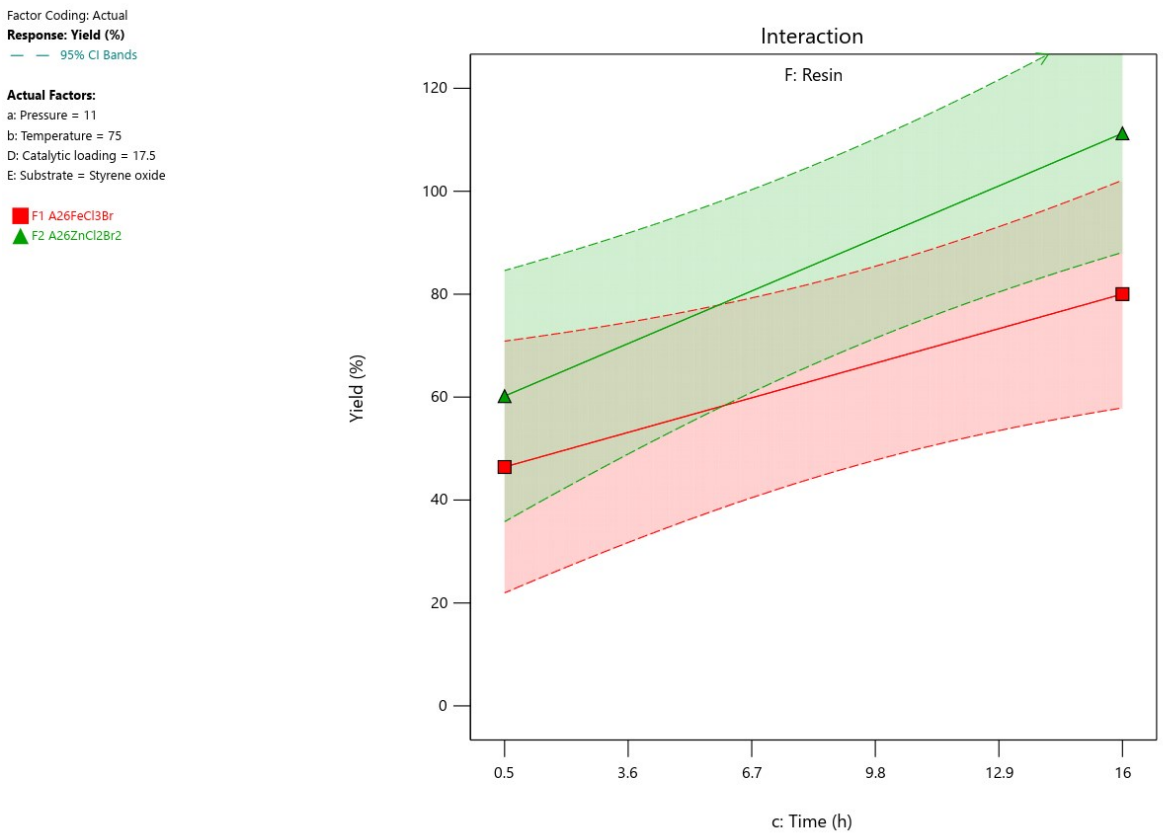

Figure S 21: interaction between reaction time and catalyst type, for styrene oxide

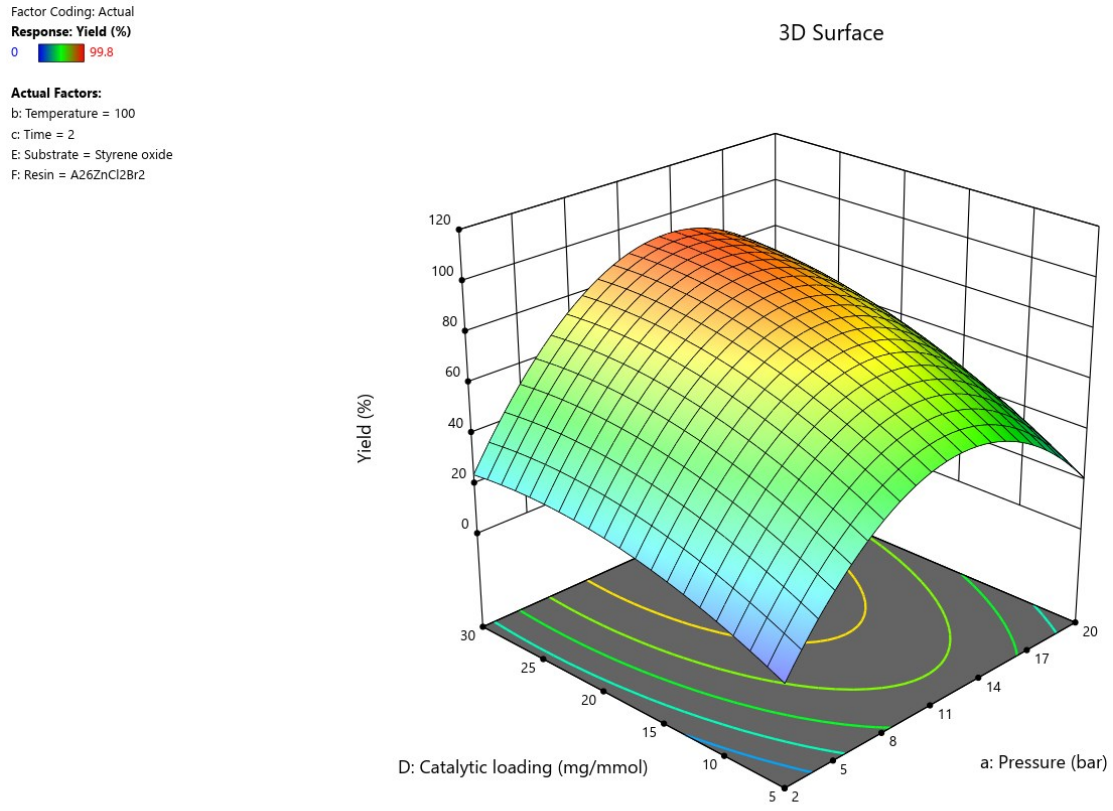

Figure S 22: interaction between catalytic loading and pressure. Yield is represented both as an axis of the graph and as a color of the surface. All the other conditions are described directly in the plot.

Factor Coding: Actual
Response: Overlay Plot
Yield
Actual Factors:
b = 94.1
c = 6.4
E = Styrene oxide
F = A26ZnCl2Br2

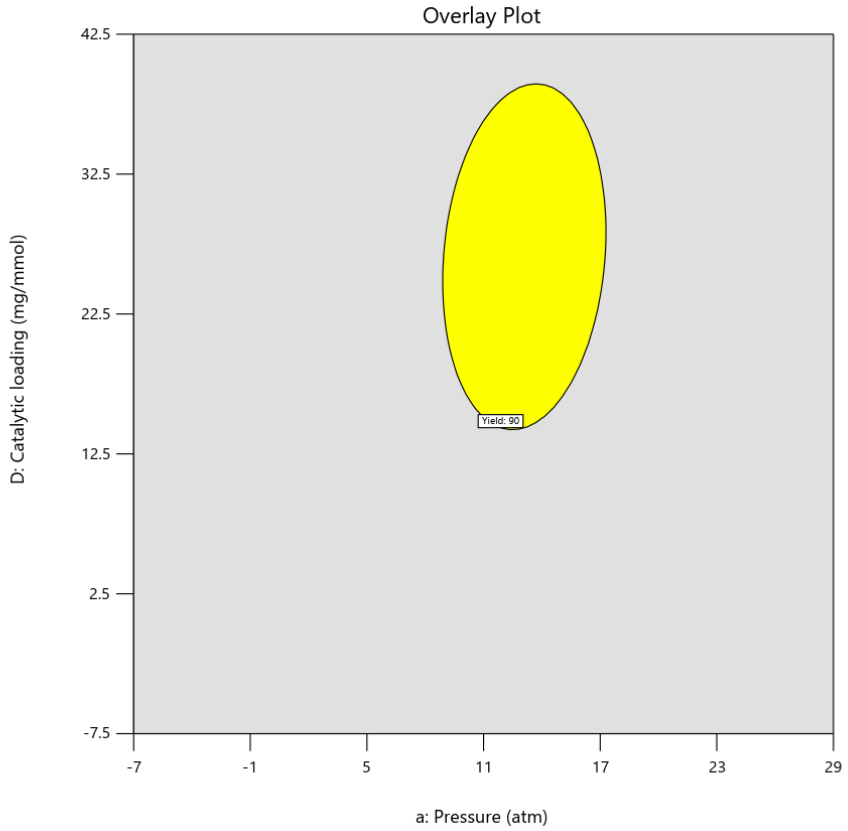

Figure S 23: the yellow area delimits the conditions needed to obtain >90% yield for styrene oxide with 6.4 hours of reaction time at 94°C

Factor Coding: Actual
Response: Overlay Plot
Yield
Actual Factors:
b = 97.8
c = 6.7
E = Propylene oxide
F = A26ZnCl2Br2

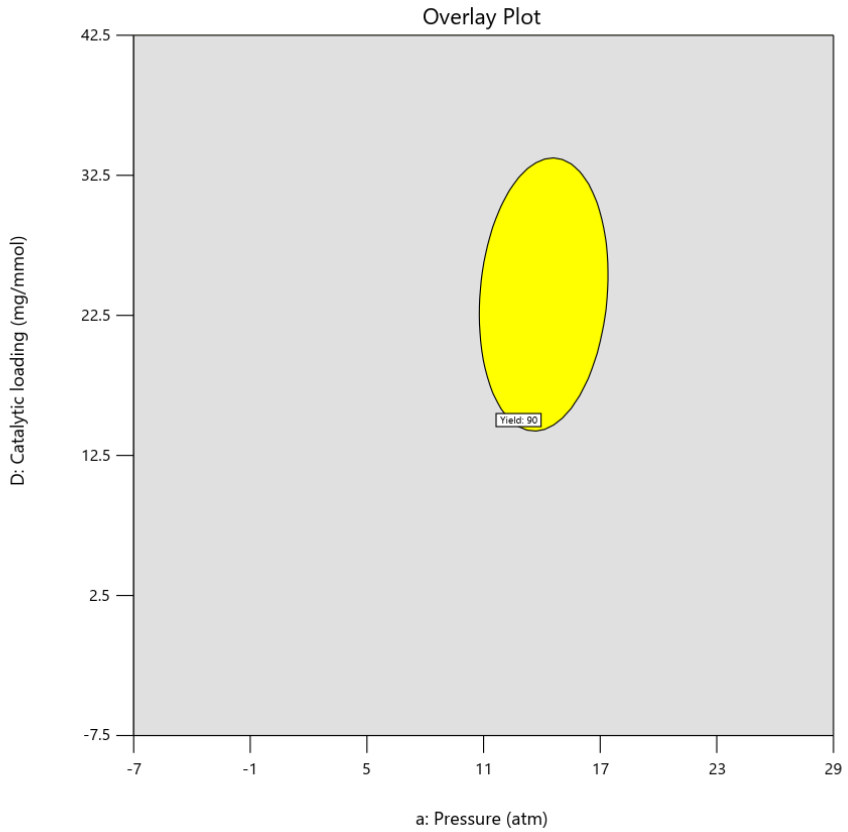

Figure S 24: the yellow area delimits the conditions needed to obtain >90% yield for propylene oxide with 6.7 hours of reaction time at 98°C

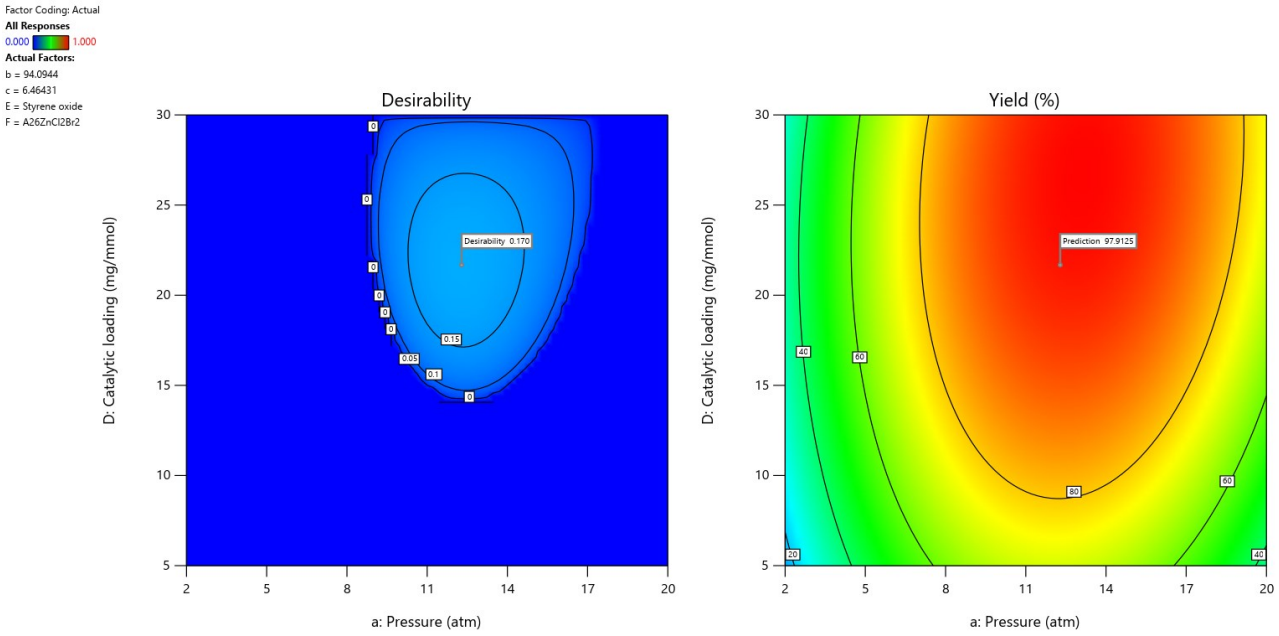

Figure S 25: desirability map for styrene oxide, along with the predicted yield. The two quadratic factors (pressure and loading) are the axis

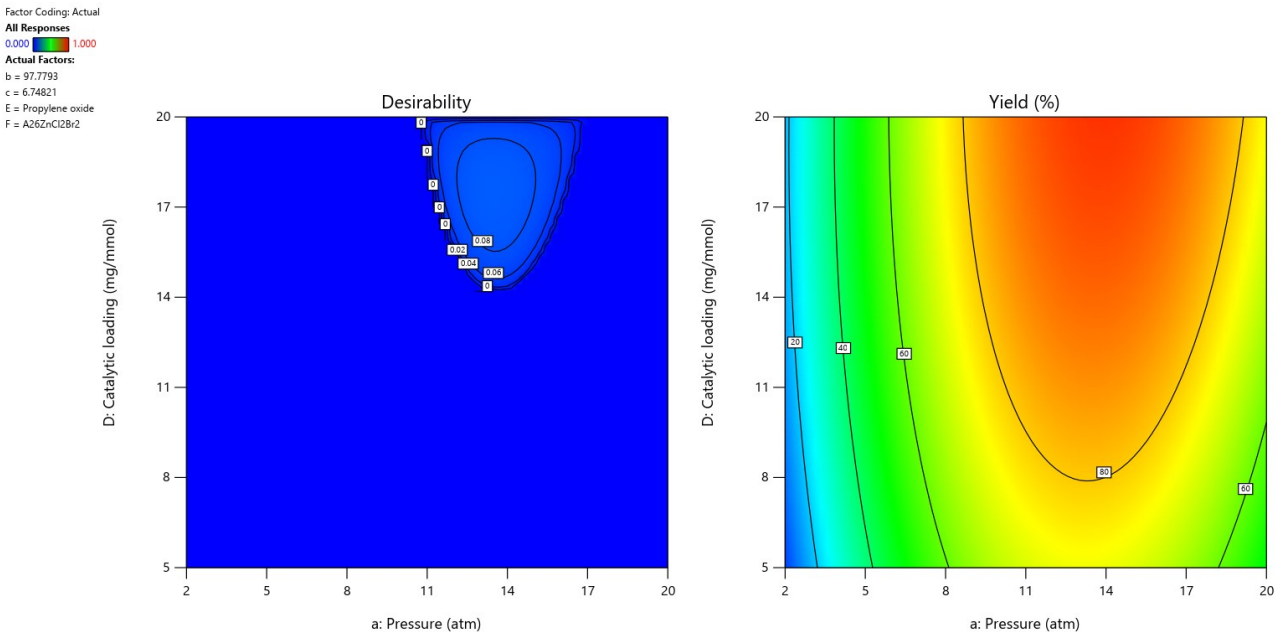

Figure S 26: desirability map for propylene oxide, along with the predicted yield. The two quadratic factors (pressure and loading) are the axis

Validation of the model, control experiments, and optimized conditions

To validate the optimization model, experiments were carried out varying the parameters and comparing the experimental yield to the theoretical yield calculated by the model. The reactions were carried out according to general procedure. Yield and conversion were calculated via fast GC-FID analysis.

Propylene oxide

Table S 9: Validation runs carried out on propylene oxide. The first run refers to the control experiment, using the unfunctionalized resin in its bromide form. Red-colored runs are highlighted as possible outliers. All runs but the ones reported in red are inside the error range of the model

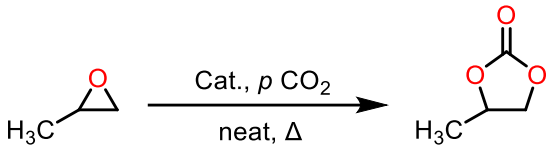

Time (h)	T (°C)	p CO_2 (MPa)	Resin	Catalytic loading (mg/mmol)	Experimental Yield (%)	Calculated Yield (%)
3.16	99	1.9	A26 Br^-	22	76.9	-
3.16	99	1.9	A26 $FeCl_3Br$	22	12.7	84.5
3.16	99	1.9	A26 $ZnCl_2Br_2$	22	100.0	78.5
0.5	98	1.9	A26 $FeCl_3Br$	24	75.0	85.6
0.5	98	1.9	A26 $ZnCl_2Br_2$	24	81.2	75.3
15.6	99	0.9	A26 $FeCl_3Br$	17.7	85.9	85.3
15.6	99	0.9	A26 $ZnCl_2Br_2$	17.7	97.3	95.8
1	100	1.4	A26 $ZnCl_2Br_2$	28	96.4	91.5
2	100	1.4	A26 $ZnCl_2Br_2$	28	44.1	92.5
2	100	1.6	A26 $ZnCl_2Br_2$	28	100.0	91.0
2	100	1.6	A26 $ZnCl_2Br_2$	17.7	100.0	85.4

Styrene oxide

Table S 10: Validation runs carried out on styrene oxide. The penultimate run is in optimized conditions. The last run is the control experiment. Results are comprised inside the model error.

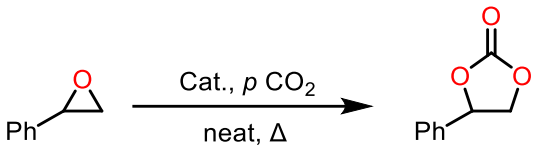

Time (h)	T (°C)	p CO_2 (MPa)	Resin	Loading (mg/mmol)	Conversion (%)	Exper. yield (%)	Calc. Yield (%)
15.6	99	0.9	**1b**, A26 $ZnCl_2Br_2$	10	95.8	91.9	>100
15.6	99	0.9	**2b**, A26 $FeCl_3Br$	10	93.7	81.7	77.5
6.5	94	1.2	**1b**, A26 $ZnCl_2Br_2$	21.6	100	100	97.9
6.5	94	1.2	**A26-Br**	21.6	64	58	-

Recycling

The zinc-functionalized resin was recycled 5 times in the CO_2 addition reaction to propylene oxide before it lost its catalytic activity, probably due to passivation of the resin's surface by the reaction product (Table S

11). The resin was recovered by filtration and then washed 3 times with 10 mL of dichloromethane. In this case, since the reactions were carried out on a higher scale, we determined the purity of the product by fast GC-FID analysis, diluting a known amount of the reaction mixture in the appropriate concentration range and adding the internal standard. Yield was then calculated from the theoretical grams of carbonate that would be obtained from a 100% yield. These runs were performed with the optimized conditions for propylene epoxide, except for the reaction time, which was reduced to 2 hours, as the reaction consistently proceeded to completion in just two hours. The spent catalyst was analyzed via SEM-EDS to evaluate its composition (Figure S 28). The zinc percentage, compared to chlorine and bromine, was found to be reduced.

Procedure. The resin (1.5 g) and 5g of propylene oxide (86 mmol) were mixed in a stainless-steel Parr autoclave. The autoclave was loaded with 1.4 MPa of CO_2 and heated at 100°C. After 2 hours, the autoclave was cooled at 0°. The resin was recovered by filtration and washed 3 times with 5 mL of dichloromethane. Yield was calculated via fast GC-FID analysis.

*Table S 11: Catalyst recycling. All reactions were carried out using the **1b**, A26 $ZnCl_2Br_2$ resin as the catalyst, at 100°C, 1.4 MPa of CO_2 pressure, for 2 hours and on 5 g of substrate (86 mmol).*

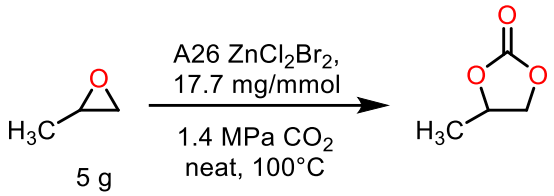

N° recycle	Yield (%)
/	96.3
1	98.0
2	94.1
3	94.9
4	92.9
5	46.7

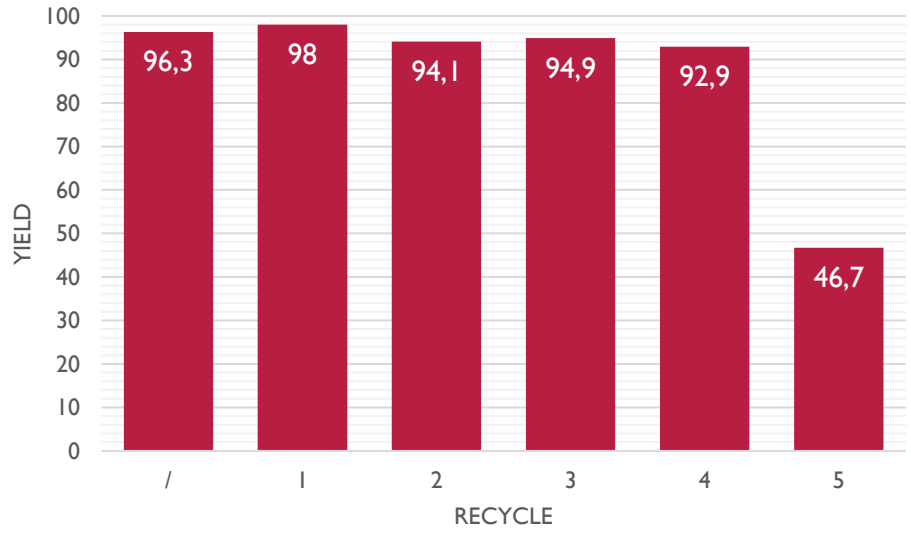

Figure S 27: Catalyst recycling. Bar graph

Catalyst stability

SEM-EDS. After the last cycle, the spent catalyst composition was analyzed with SEM-EDS spectroscopy

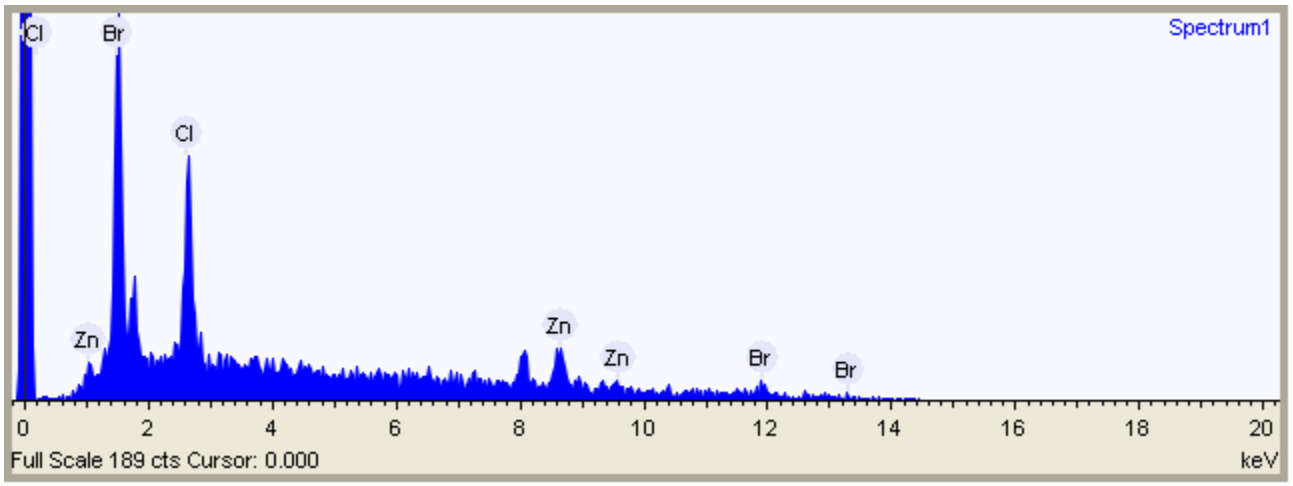

*Figure S 28: EDS spectrum of spent **1b**, A26 $ZnCl_2Br_2$*

Element	Weight %
Chlorine	29.2
Zinc	8.1
Bromine	62.8

Differential Scanning Calorimetry (DSC).

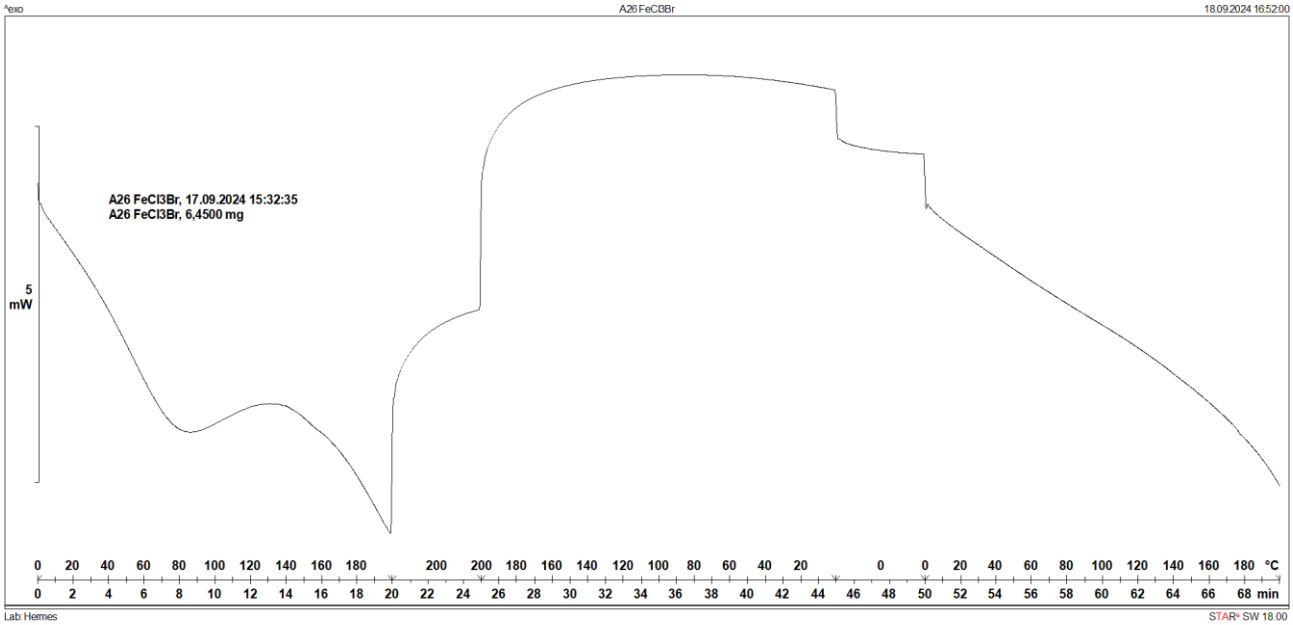

*Figure S 29: DSC measurement of **2b**, A26 $FeCl_3Br$*

DSC analysis of the sample **2b**, A26-$FeCl_3Br$ (temperature program 0°C-200°C [10°C/min]-0°C [-10°C/min]-200°C [10°C/min]) indicates the absence of any particular glass transition of the material or any melting point, which is expected for a cross-linked polystyrene. The heat change in the first section of the curve can be

attributed to the loss of residual solvents, and possibly to a broad and irregular rearrangement of the polystyrene chains.

In the second 0°C-200°C step, the first section of the curve related to solvent loss is therefore missing, confirming this hypothesis.

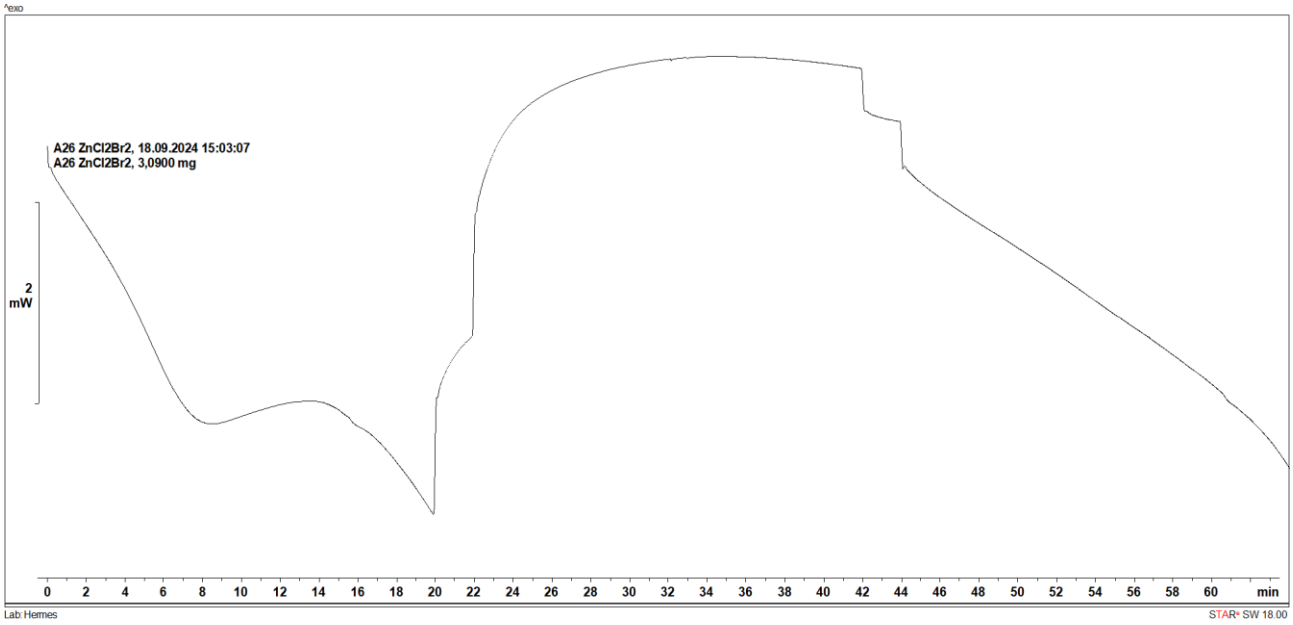

Figure S 30: DSC measurement of ***1b****, A26 $ZnCl_2Br_2$*

The support is the same and the presence of the metal does not strongly affect the curve.

Even in this case, the first section of the curve shows the evaporation of residual solvent, which is then missing in the second 0-200°C section.

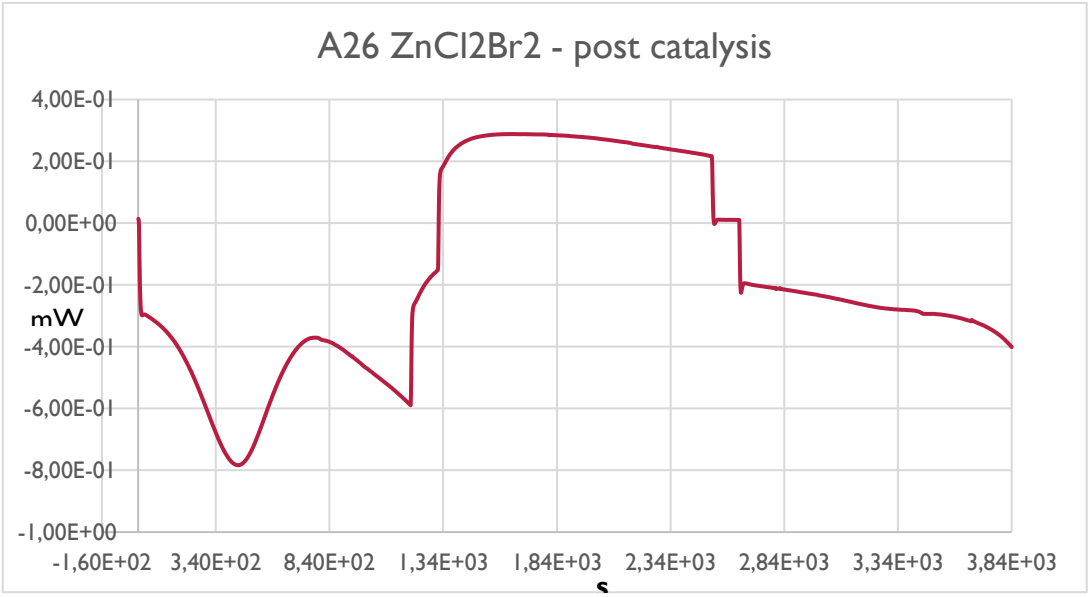

Figure S 31: DSC measurement of ***1b****, A26 $ZnCl_2Br_2$ post-catalysis.*

DSC measurements were repeated on spent catalysts after five runs. A part from a major heat change in the first section of the curve, which can be attributed to organic residues, the curve is essentially unchanged and identical in the second run, showing the stability of the material.

Thermogravimetric analysis (TGA).

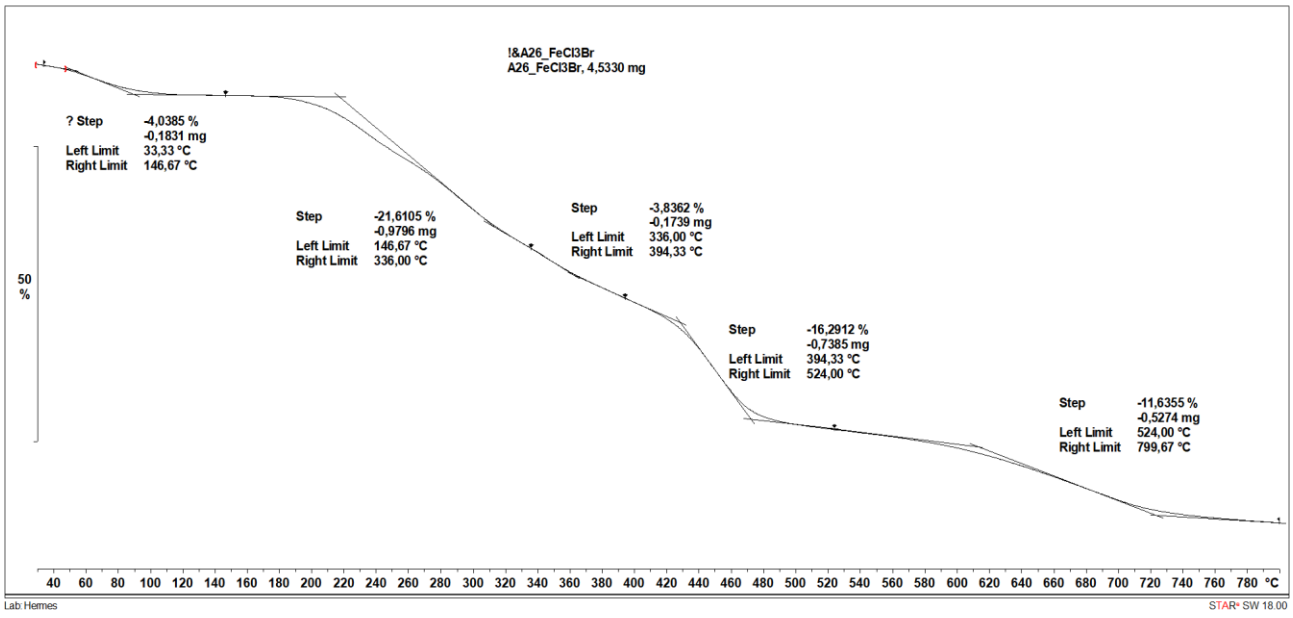

Figure S 32: TGA measurement of ***2b****, A26 $FeCl_3Br$*

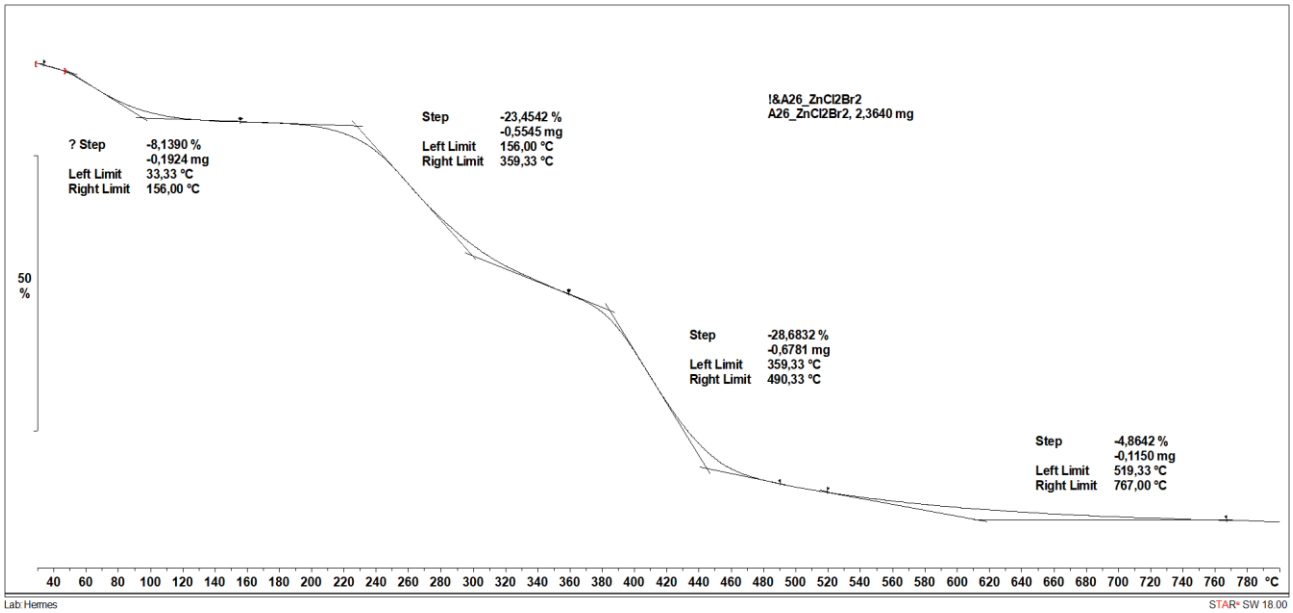

Figure S 33: TGA measurement of ***1b****, A26 $ZnCl_2Br_2$*

In the range 30-800 ° C, for both samples **2b**, A26-$FeCl_3Br$ and **1b**, A26-$ZnCl_2Br_2$, we can confirm the initial loss of residual solvents and the stability of the material until over 150°C. After this point, both samples show a significant mass reduction due to the degradation of the polymeric material. In particular, we have noticed a strong amine smell resulting from the heating of the material, so we can assume that the ammonium functionalities are the first to be degraded during thermal treatment over 150°C. Therefore, we can assume in general that at the common reaction temperature (rt-100°C) the catalysts are stable.

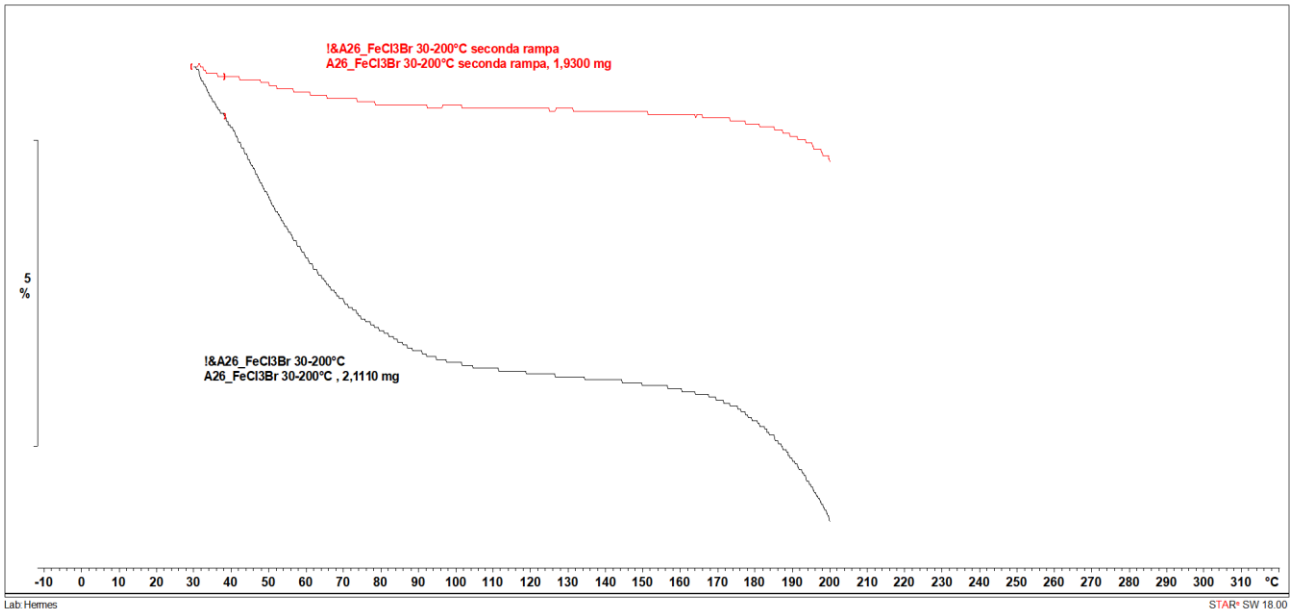

Figure S 34: comparison between TGA measurement of ***2b****, A26 $FeCl_3Br$ first run (black curve) and second run (red curve)*

To further confirm the initial loss of residual solvent, we performed a 30-200°C run twice of the sample **2b**, A26-$FeCl_3Br$, in which we can see the difference in mass loss in the first run (black curve) and the almost absence of any mass variation in the second run (red curve).

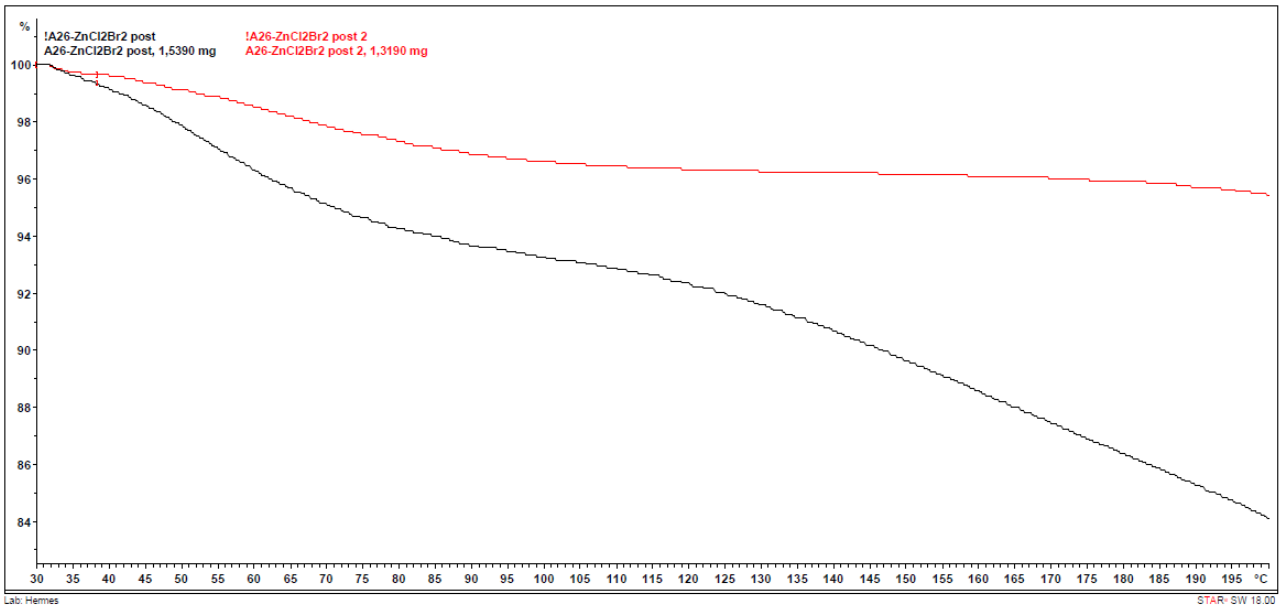

Figure S 35: comparison between TGA measurement of spent ***1b****, A26 $ZnCl_2Br_2$ post-catalysis, first run (black curve) and second run (red curve)*

IR comparison between fresh and spent catalyst

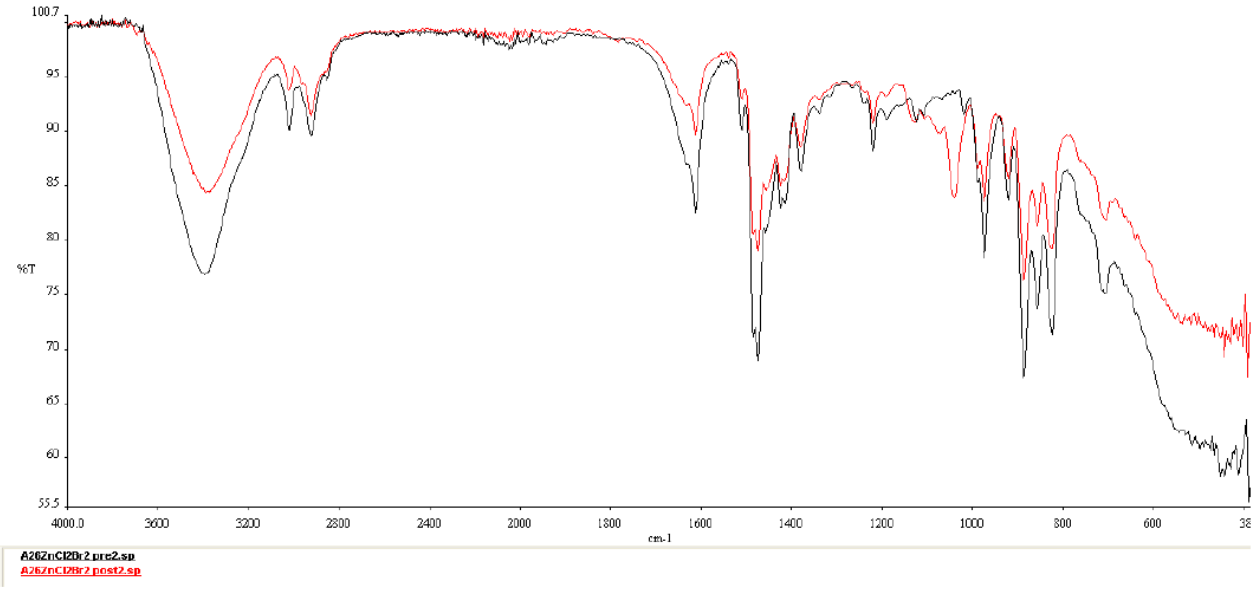

Figure S 36: comparison between IR spectra of fresh ***1b****, A26 $ZnCl_2Br_2$, (black curve) and spent* ***1b****, A26 $ZnCl_2Br_2$ post-catalysis (red curve)*

Reaction scope

The reaction was carried out on different substrates according to general procedure, with the following conditions: T = 100°C, p_{CO_2} = 1.4 MPa, time: 2 h, catalyst: A26 $ZnCl_2Br_2$ (17.7 mg/mmol).

*Table S 12: Reaction scope. All reactions were carried out using the **1b**, A26 $ZnCl_2Br_2$ resin as the catalyst, at 100°C, 1.4 MPa of CO_2 pressure, for 2 hours.*

Substrate	Product	Yield
3d, 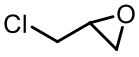	**4d,** 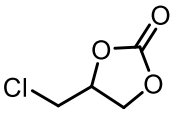	100% (isolated)
3e, 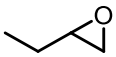	**4e,** 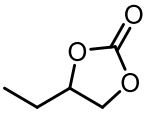	95.5% (isolated)
3f, 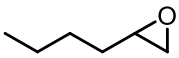	**4f,** 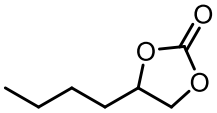	66% (NMR)
3g, 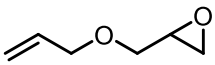	**4g,** 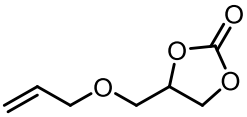	53.8% (NMR)
3h, 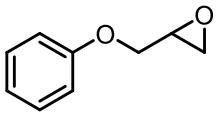	**4h,** 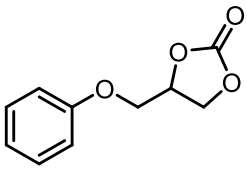	98.7% (isolated)
3i, 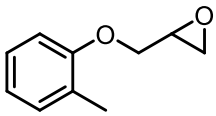	**4i,** 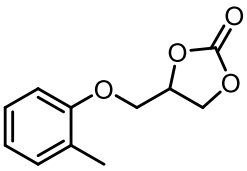	51.3% (isolated)
3j, 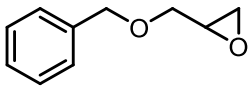	**4j,** 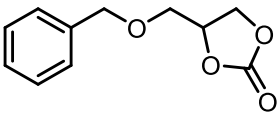	66.8% (NMR)
3k, 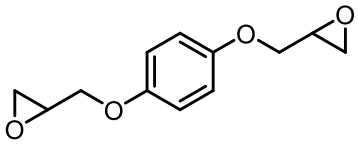	**4k,** 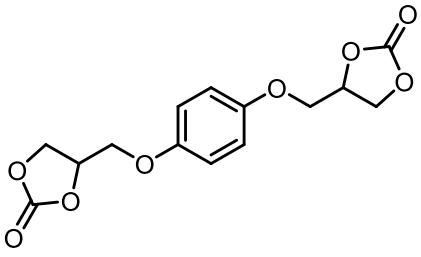	85.7% (NMR) 83.2% (isolated)
3l, 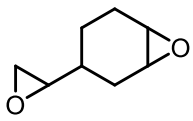	**4l,** 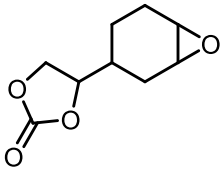	9.7% (NMR)
3m, 	**4m,** 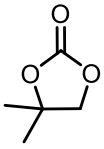	0% (NMR)

Products' characterization

***4a**, propylene carbonate*

^{1}H-NMR: δ 4.91–4.83 (m, 1H), 4.59–4.55 (t, J = 8 Hz, 1H), 4.06–4.02 (t, J = 8 Hz, 1H), 1.52–1.51 (t, J = 4 Hz, 3H). The data is in agreement with the literature.[1]

***4b**, styrene carbonate*

^{1}H-NMR: δ 7.50–7.37 (m, 5H), 5.72–5.68 (t, J = 8 Hz, 1H), 4.84–4.80 (t, J = 8 Hz, 1H), 4.39–4.35 (t, J = 4 Hz, 1H). The data is in agreement with the literature.[1]

***4c**, cyclohexene carbonate*

^{1}H-NMR: δ 4.72–4.67 (m, 5H), 1.94–1.63 (t, J = 8 Hz, 4H), 1.61–1.58 (m, 2H), 1.50–1.40 (m, 2H). The data is in agreement with the literature.[1]

***4d**, 4-chloromethyl-[1,3]-dioxolan-2-one*

The resin (catalyst loading = 17.7 mg/mmol) and 500 mg of epichlorohydrin (5.4 mmol) were mixed together in an autoclave vial capped with a septum. The autoclave was loaded with 1.4 MPa of CO_2, and heated at 100°C. After 2 hours, the autoclave was cooled at 0°C to quench the reaction. The reaction mixture was filtered to remove the resin. No further purification was needed.

^{1}H-NMR: δ 5.00–4.94 (m, 1H), 4.63–4.59 (t, J = 8 Hz, 1H), 4.45–4.41 (m, 1H), 3.78–3.76 (m, 2H)

^{13}C NMR: δ 154.03 (s, 1C), 74.19 (s, 1C), 66.98 (s, 1C), 43.49 (s, 1C)

The data is in agreement with the literature.[1]

***4e**, butylene carbonate*

The resin (catalyst loading = 17.7 mg/mmol) and 500 mg of 1,2 epoxybutane (6.93 mmol) were mixed together in an autoclave vial capped with a septum. The autoclave was loaded with 1.4 MPa of CO_2, heated at 100°C. After 2 hours, the autoclave was cooled at 0°C to quench the reaction. The reaction mixture was filtered to remove the resin. No further purification was needed.

^{1}H-NMR: δ 4.71–4.64 (m, 1H), 4.56–4.52 (t, J = 8 Hz, 1H), 4.12–4.08 (t, J = 8 Hz, 1H), 3.88–3.77 (m, 2H; partially overlapping with epoxide's signals), 1.07–1.03 (t, J = 8 Hz, 3H; partially overlapping with epoxide's signals)

The data is in agreement with the literature.[1]

***4f**, hexylene carbonate*

The resin (catalyst loading = 17.7 mg/mmol) and 500 mg of 1,2 epoxyhexane (4.99 mmol) were mixed together in an autoclave vial capped with a septum. The autoclave was loaded with 1.4 MPa of CO_2 and heated at 100°C. After 2 hours, the autoclave was cooled at 0°C to quench the reaction. The product was purified by chromatographic column (hexane : ethyl acetate = 8 : 2)

^{1}H-NMR: δ 4.76–4.69 (m, 1H), 4.57–4.52 (t, J = 8 Hz, 1H), 4.11–4.07 (m, 1H), 1.89–1.80 (m, 1H), 1.76–1.67 (m, 1H), 1.60–1.38 (m, 4H; overlapping with the epoxide's signals)

The data is in agreement with the literature.[1]

***4g**, 4 allyloxymethyl [1,3] dioxolan 2-one*

The resin (catalyst loading = 17.7 mg/mmol) and 500 mg of allyl glycidyl ether (4.38 mmol) were mixed together in an autoclave vial capped with a septum. The autoclave was loaded with 1.4 MPa of CO_2 and

[1] J. Steinbauer, A. Spannenberg,; T. Werner, *Green Chemistry*, **2017**, *19*, 3769-3779.

heated at 100°C for 2 hours. After 2 hours, the autoclave was cooled at 0°C to quench the reaction. The product was purified by chromatographic column (hexane : ethyl acetate = 6 : 4)

^{1}H-NMR: δ 6.00–5.86 (m, 1H), 5.36–5.22 (m, 2H; overlapping with the epoxide's signals), 4.87–4.81 (m, 1H), 4.55–4.42 (m, 2H), 4.11–4.07 (m, 2H; overlapping with the epoxide's signals), 3.78–3.64 (m, 2H; overlapping with the epoxide's signals)

The data is in agreement with the literature.[1]

***4h**, 4-phenyloxymethyl [1,3] oxolan 2 one*

The resin (catalyst loading = 17.7 mg/mmol) and 500 mg of phenyl glycidyl ether (3.33 mmol) were mixed together in an autoclave vial capped with a septum. The autoclave was loaded with 1.4 MPa of CO_2 and heated at 100°C. After 2 hours, the autoclave was cooled at 0°C to quench the reaction. The product at the end of the reaction precipitated as white crystals. The resin was filtered after dissolving the product in DCM. The solvent was evaporated under reduced pressure and the product was recovered as white powder.

^{1}H-NMR: δ 7.36–6.92 (m, 5H; overlapping), 5.08–5.02 (m, 1H), 4.66–4.55 (m, 2H), 4.28–4.16 (m, 2H)

The data is in agreement with the literature.[2]

***4i**, 4-((o-tolyloxy)methyl)-[1,3]-dioxolan-2-one*

The resin (catalyst loading = 17.7 mg/mmol) and 500 mg of 2 methyl phenyl glycidyl ether (3.04 mmol) were mixed together in an autoclave vial capped with a septum. The autoclave was loaded with 1.4 MPa of CO_2 and heated at 100°C. After 2 hours, the autoclave was cooled at 0°C to quench the reaction. The product was purified by chromatographic column (hex : AcOEt = 7 : 3).

^{1}H-NMR: δ 7.21–7.16 (m, 2H), 6.97–6.93 (m, 1H), 6.82–6.79 (m, 1H), 5.10–5.05 (m, 1H), 4.68–4.59 (m, 2H), 4.31–4.15 (m, 2H), 2.55 (s, 3H)

The data is in agreement with the literature.[2]

***4j**, 4-benzyloxymethyl [1,3] oxolan 2 one*

The resin (catalyst loading = 17.7 mg/mmol) and 500 mg of benzyl glycidyl ether (3.05 mmol) were mixed together in an autoclave vial capped with a septum. The autoclave was loaded with 1.4 MPa of CO_2 and heated at 100°C. After 2 hours, the autoclave was cooled at 0°C to quench the reaction. The product was purified by chromatographic column (hex : AcOEt = 6 : 4).

^{1}H-NMR: δ 7.40–7.33 (m, 5H; partially overlapping with the epoxide's signals), 4.86–4.81 (m, 1H), 4.67–4.57 (m, 2H; partially overlapping with the epoxide's signals), 4.53–4.48 (m, 1H), 4.43–4.39 (m, 1H), 3.76–3.63 (m, 2H; partially overlapping with the epoxide's signals)

The data is in agreement with the literature.[2]

***4k**, 4,4'-((1,4-phenylenebis(oxy))bis(methylene))bis([1,3]-dioxolan-2-one)*

The resin (catalyst loading = 17.7 mg/mmol) and 131 mg of benzyl glycidyl ether (0.59 mmol) were dissolved in 1 mL of propylene carbonate, and then mixed together in an autoclave vial capped with a septum. The autoclave was loaded with 1.4 MPa of CO_2 and heated at 100°C. After 2 hours, the autoclave was cooled at 0°C to quench the reaction. The resin was filtered away, and after adding mesitylene as the internal standard to calculate NMR yield, the product precipitated as a white solid. The carbonate was filtered to remove mesitylene and propylene carbonate and washed 3 times with 2 mL of hexane.

^{1}H-NMR: δ 6.92 (s, 4H), 5.15–5.10 (m, 2H), 4.65–4.60 (m, 2H), 4.40–4.36 (m, 2H), 4.25–4.13 (m, 4H)

---

[2] H. Ma, S. Liu, H. Wang, G. Li, K. Zhao, X. Cui, F. Shi, *Green Chemistry*, **2023**, *25*, 2293 – 2298.

The data is in agreement with the literature.[3]

***4l**, 4-(7-oxabicyclo[4.1.0]heptan-3-yl)-[1,3]-dioxolan-2-one*

The resin (catalyst loading = 17.7 mg/mmol) and 500 mg of vinylcyclohexene dioxide (3.57 mmol), were mixed together in an autoclave vial capped with a septum. The autoclave was loaded with 1.4 MPa of CO_2 and heated at 100°C. After 2 hours, the autoclave was cooled at 0°C to quench the reaction. Since the NMR yield was very low, the product wasn't further purified.

^{1}H-NMR: δ 4.52–4.47 (m, 2H), 4.20–4.14 (m, 1H), 3.23–3.16 (m, 2H; overlapped with epoxide's signals), 2.7–1 (cyclohexane ring, overlapped with the bis-epoxide's signals)

The data is in agreement with the literature.[1]

NMR spectra of the products

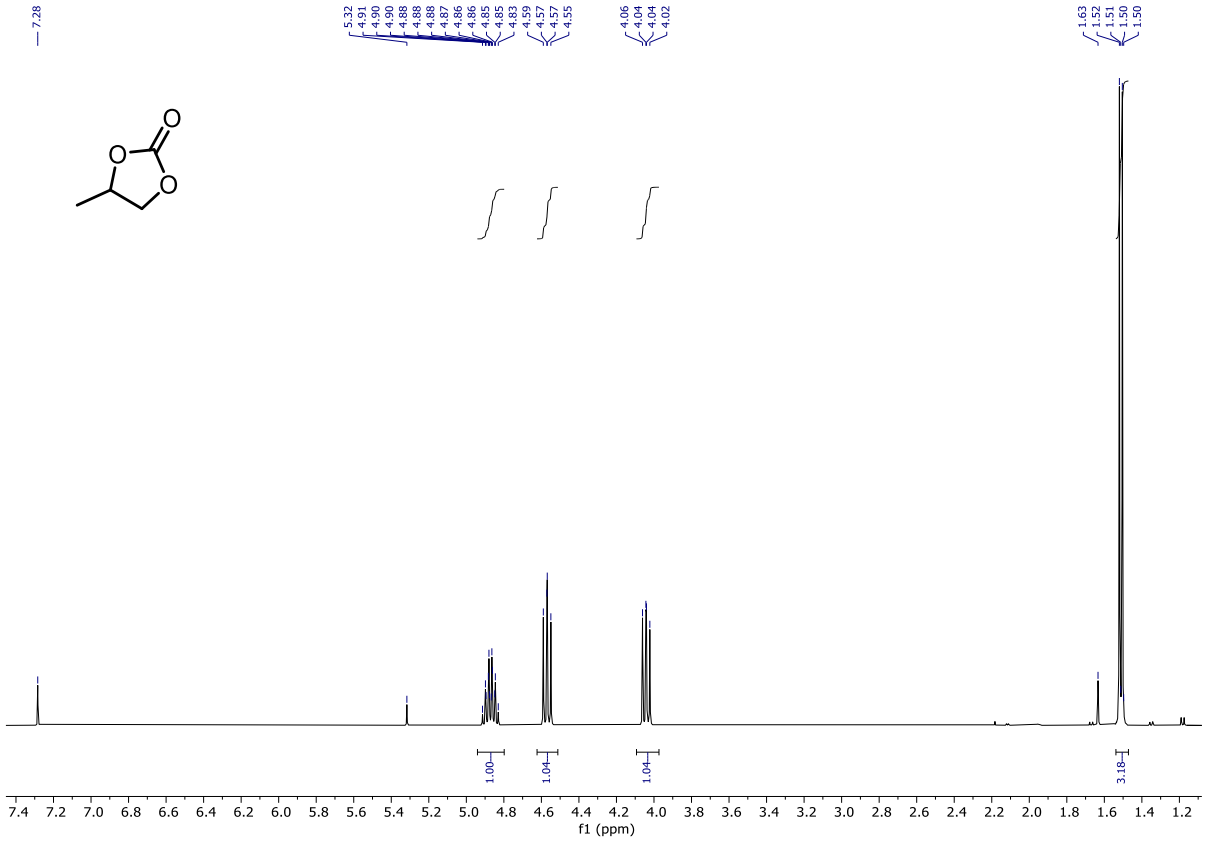

Figure S 37: ^{1}H-NMR spectra of propylene carbonate in $CDCl_3$

[3] E. A. Elgohary, Y. M. A. Mohamed, S. T. Rabie, S. A. Salih, A. M. Fekry, H. A. El Nazer, *New Journal of Chemistry*, **2021**, *45*, 17301 – 17312.

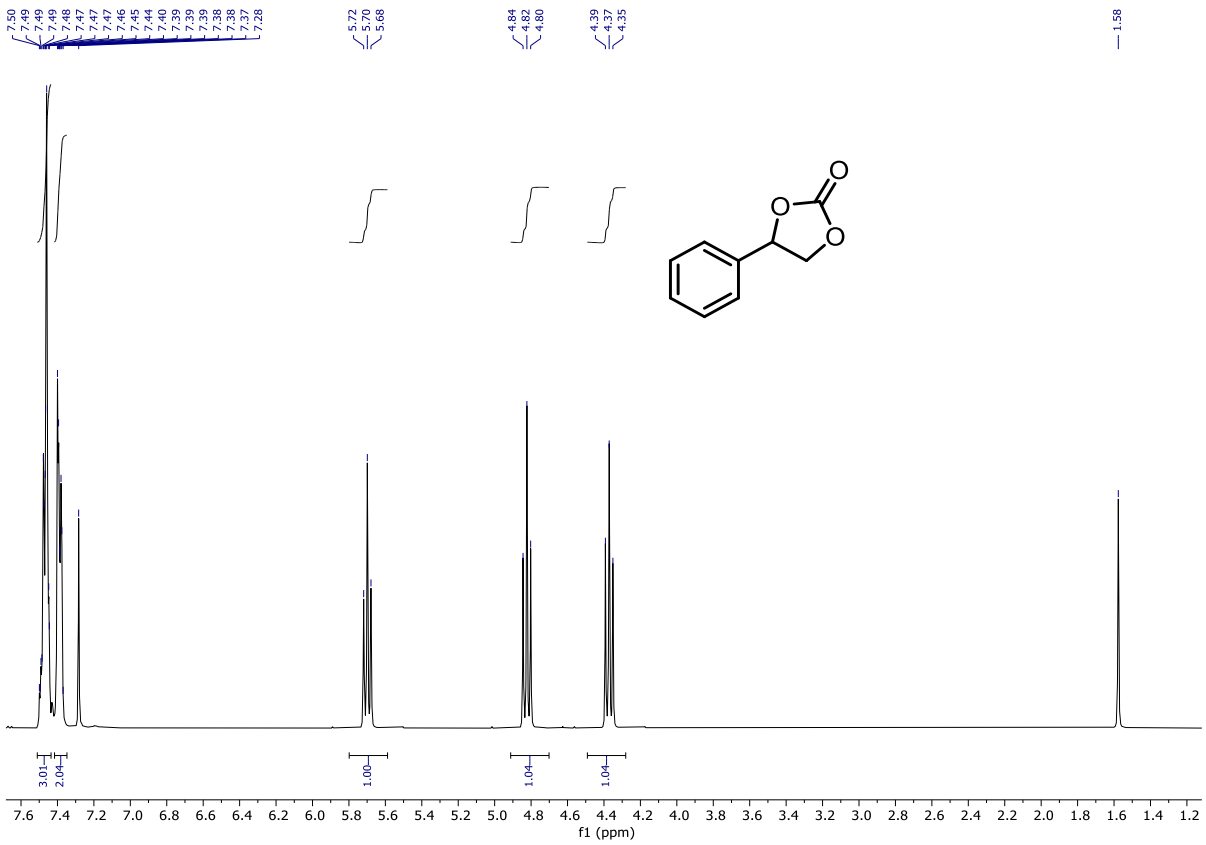

Figure S 30: ^{1}H-NMR spectra of styrene carbonate in $CDCl_3$

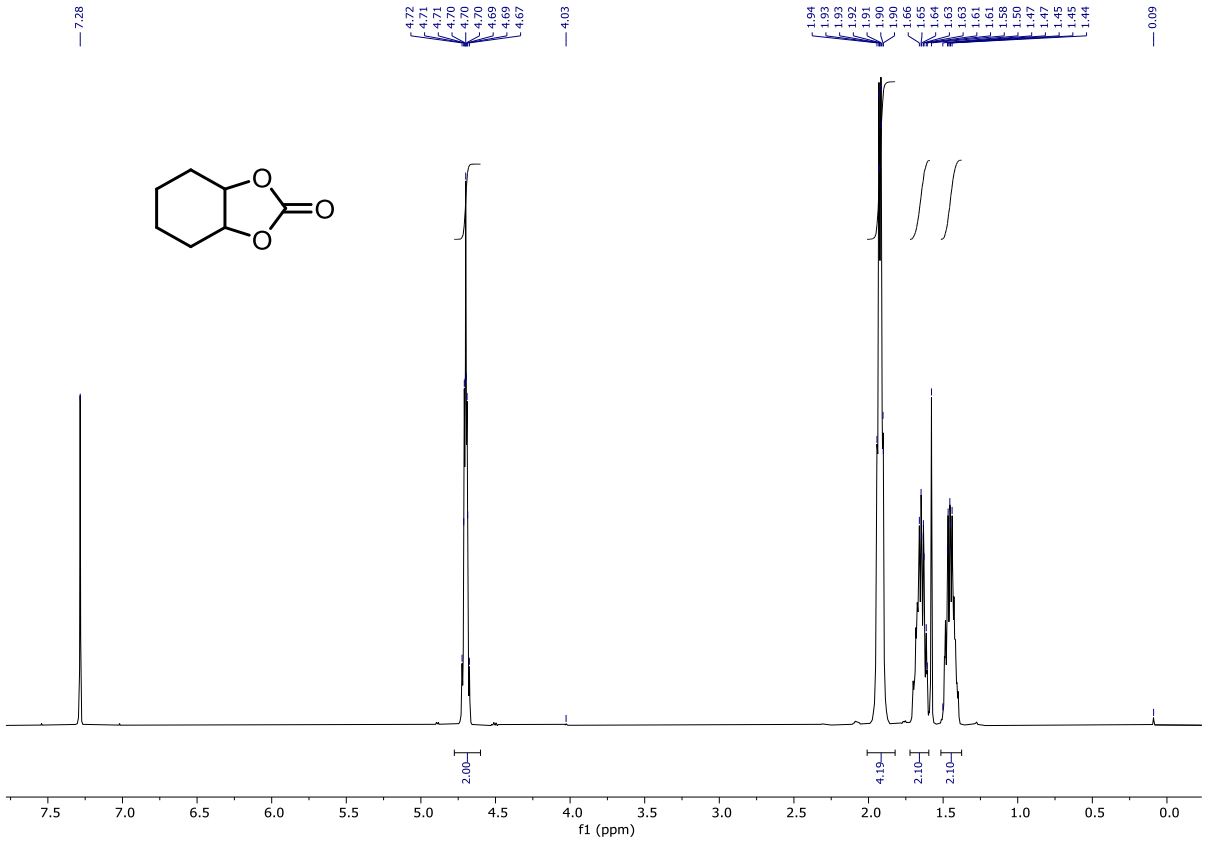

Figure S 31: ^{1}H-NMR of cyclohexene carbonate in $CDCl_3$

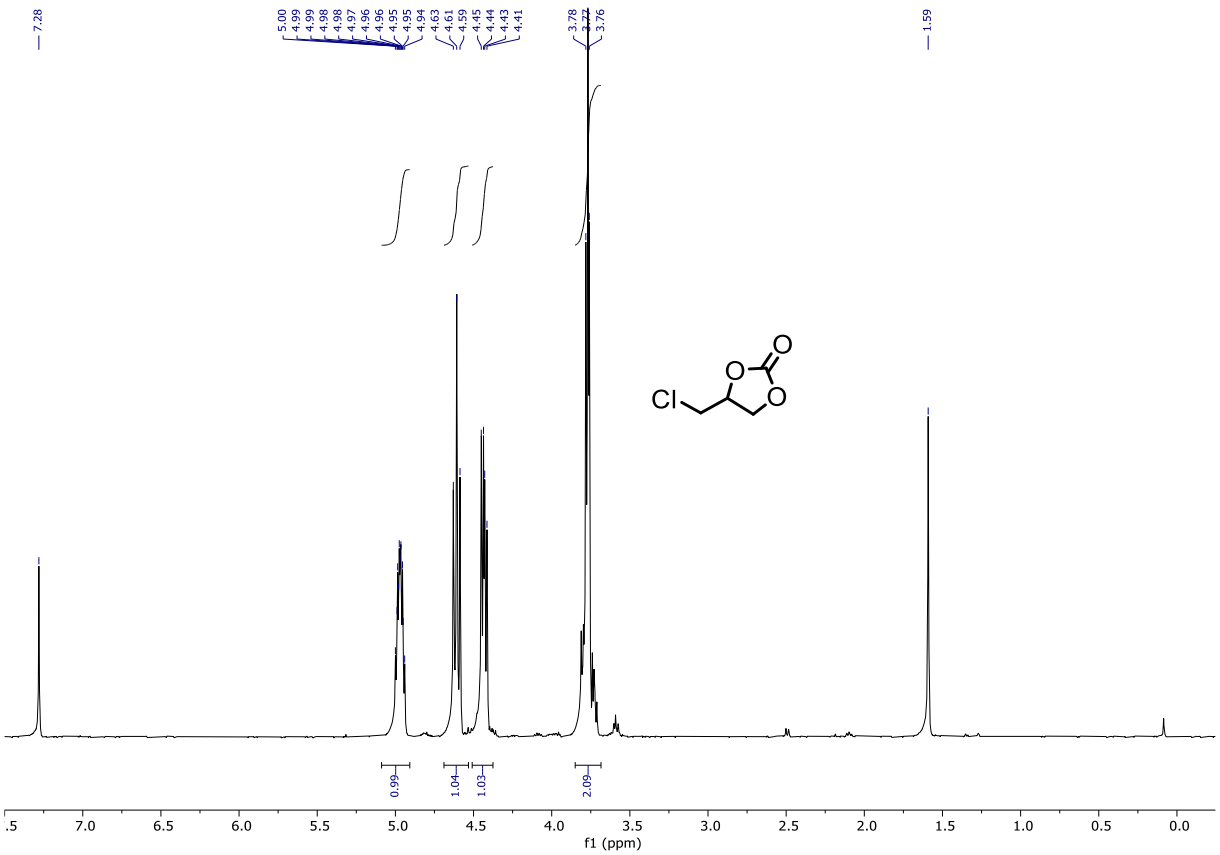

Figure S 40: ^{1}H-NMR spectra of 4-chloromethyl-[1,3]-dioxolan-2-one in $CDCl_3$

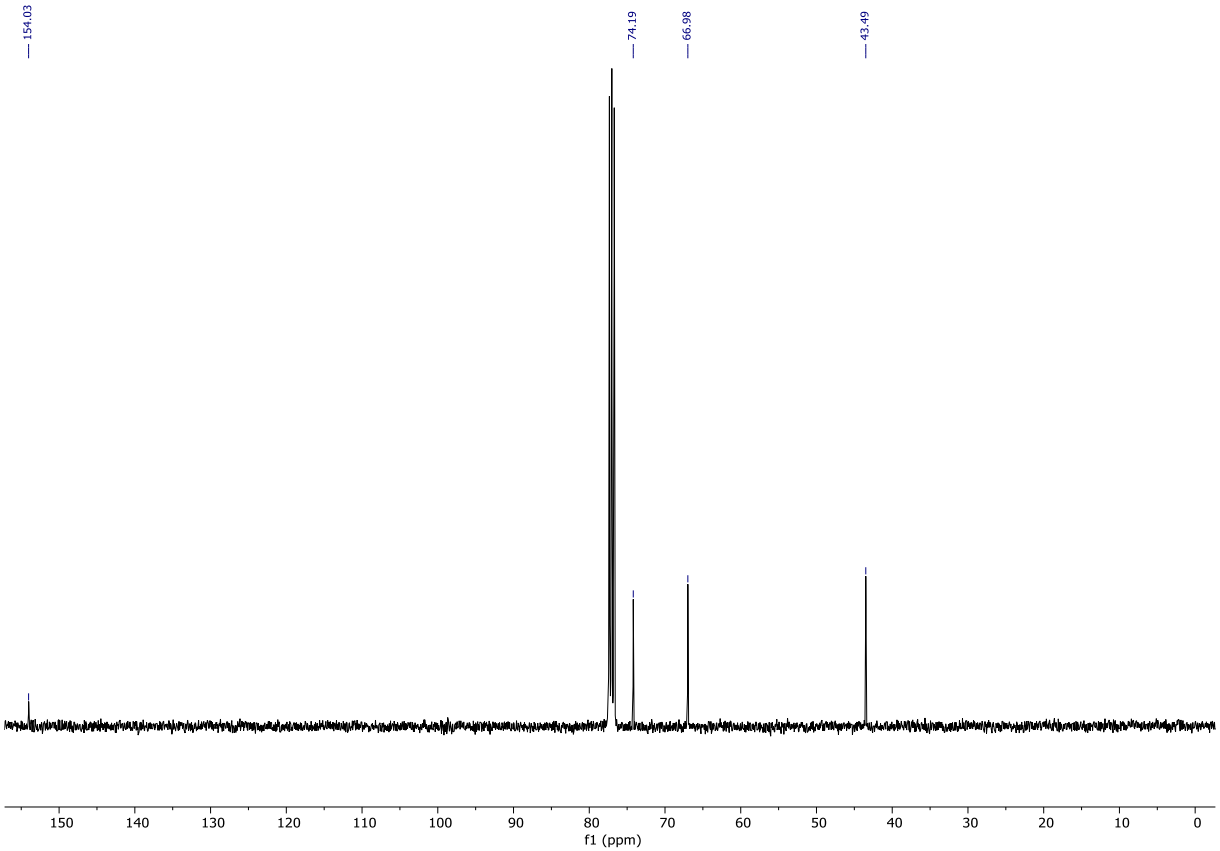

Figure S 41: ^{13}C-NMR spectra of 4-chloromethyl-[1,3]-dioxolan-2-one in $CDCl_3$ in $CDCl_3$

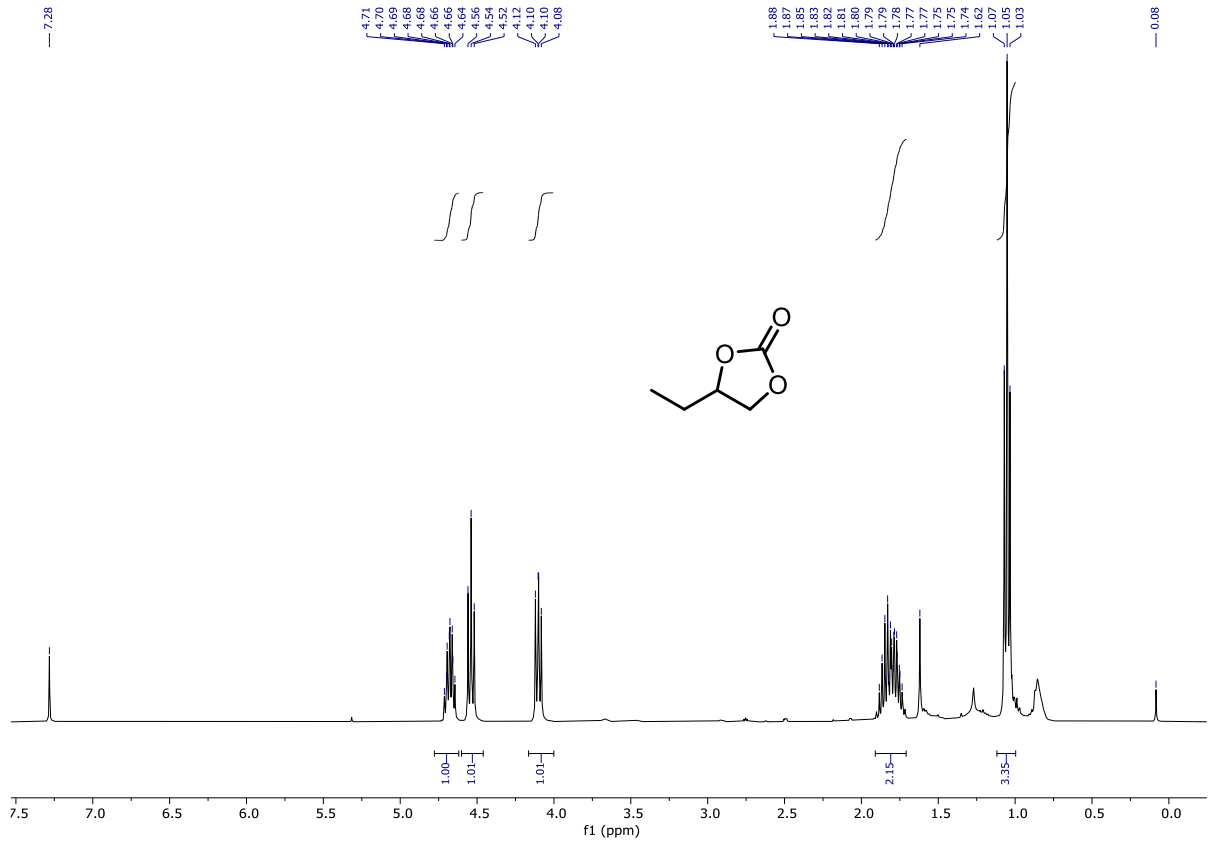

Figure S 42: ^{1}H-NMR spectra of butylene carbonate in $CDCl_3$

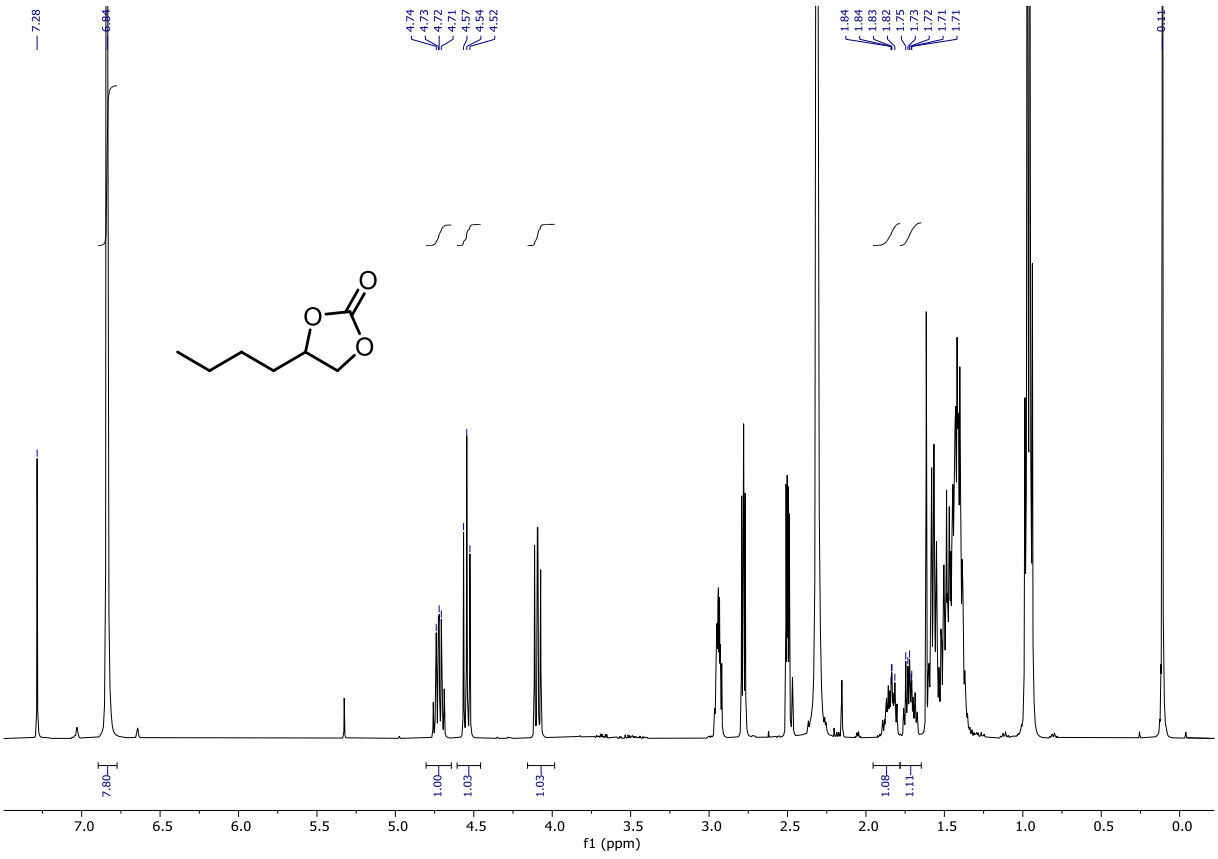

Figure S 43: ^{1}H-NMR of 1,2-hexylene carbonate (reaction crude + mesitylene) in $CDCl_3$

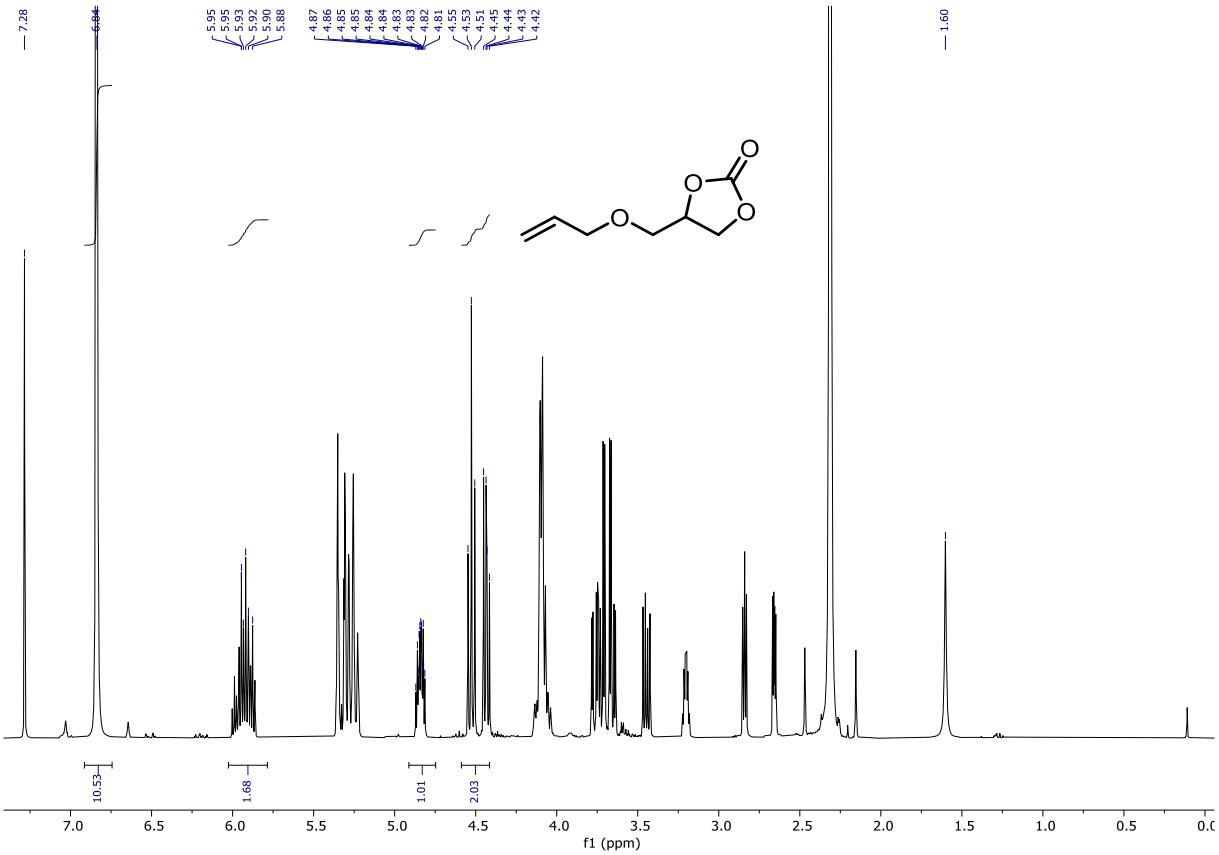

Figure S 44: ^{1}H-NMR of 4-allyloxymethyl 1,3-dioxolan-2-one (reaction crude + mesitylene) in $CDCl_3$

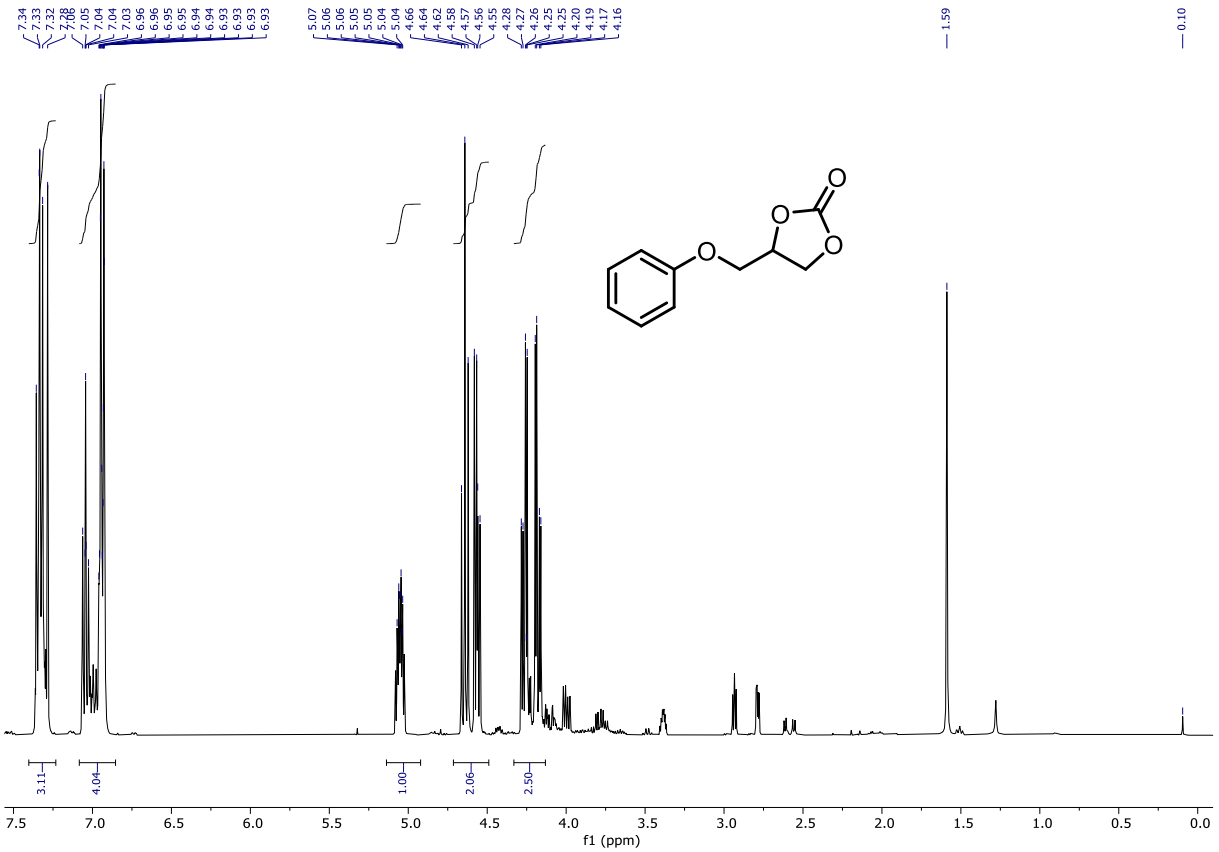

Figure S 45: ^{1}H-NMR spectra of 4-phenyloxymethyl-[1,3]-oxolan-2-one in $CDCl_3$

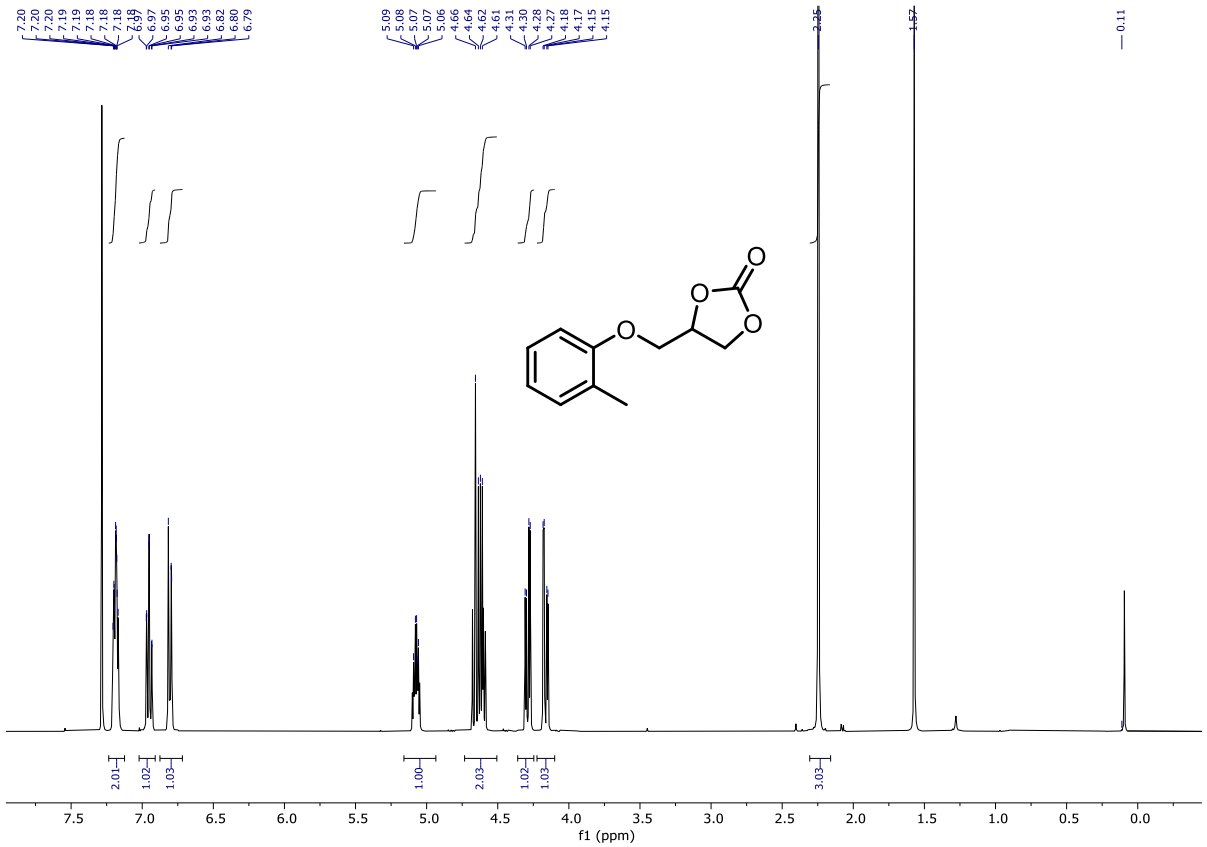

Figure S 46: ^{1}H-NMR spectra of 4-((o-tolyloxy)methyl)-1,3-dioxolan-2-one in $CDCl_3$

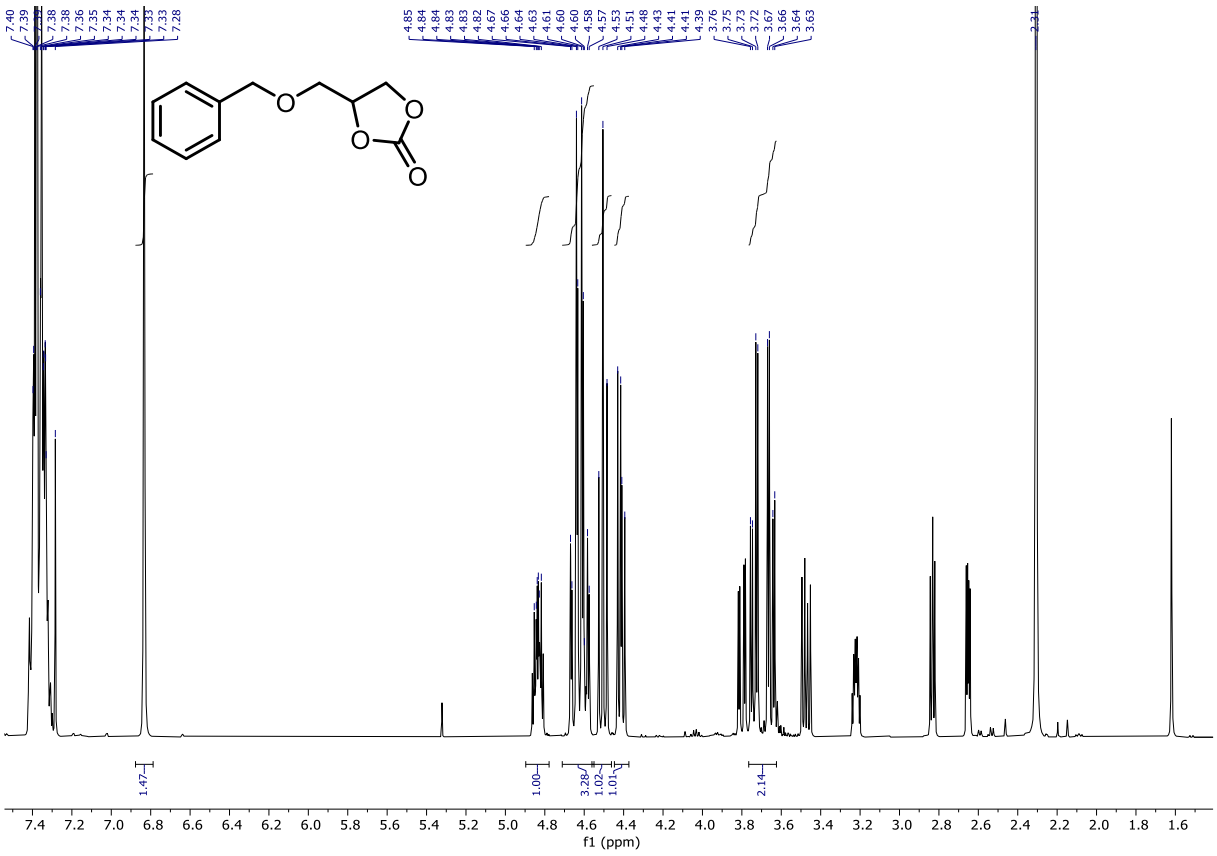

Figure S 47: ^{1}H-NMR spectra of 4-benzyloxymethyl-[1,3]-oxolan-2-one (reaction crude + mesitylene) in $CDCl_3$

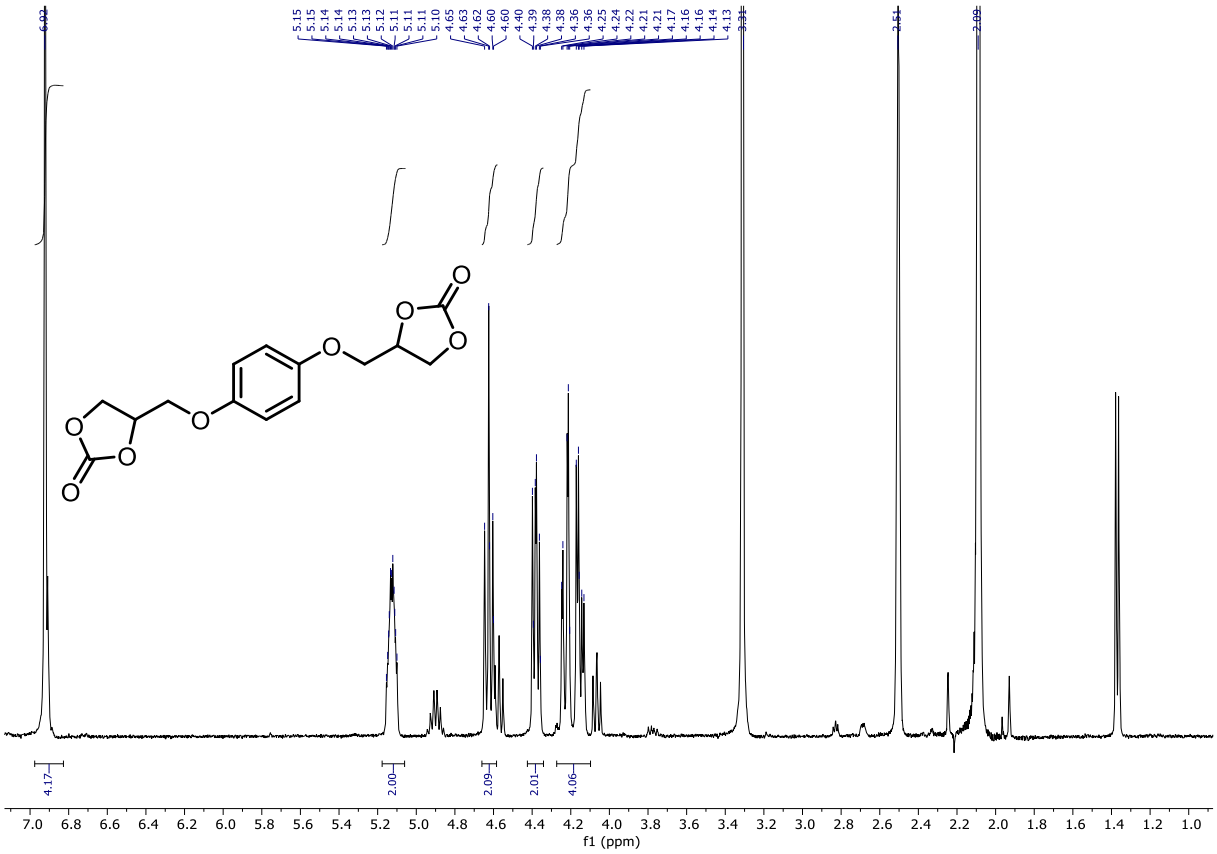

Figure S 48: ^{1}H-NMR spectra of 4,4'-((1,4-phenylenebis(oxy))bis(methylene))-bis(1,3-dioxolan-2-one) in DMSO

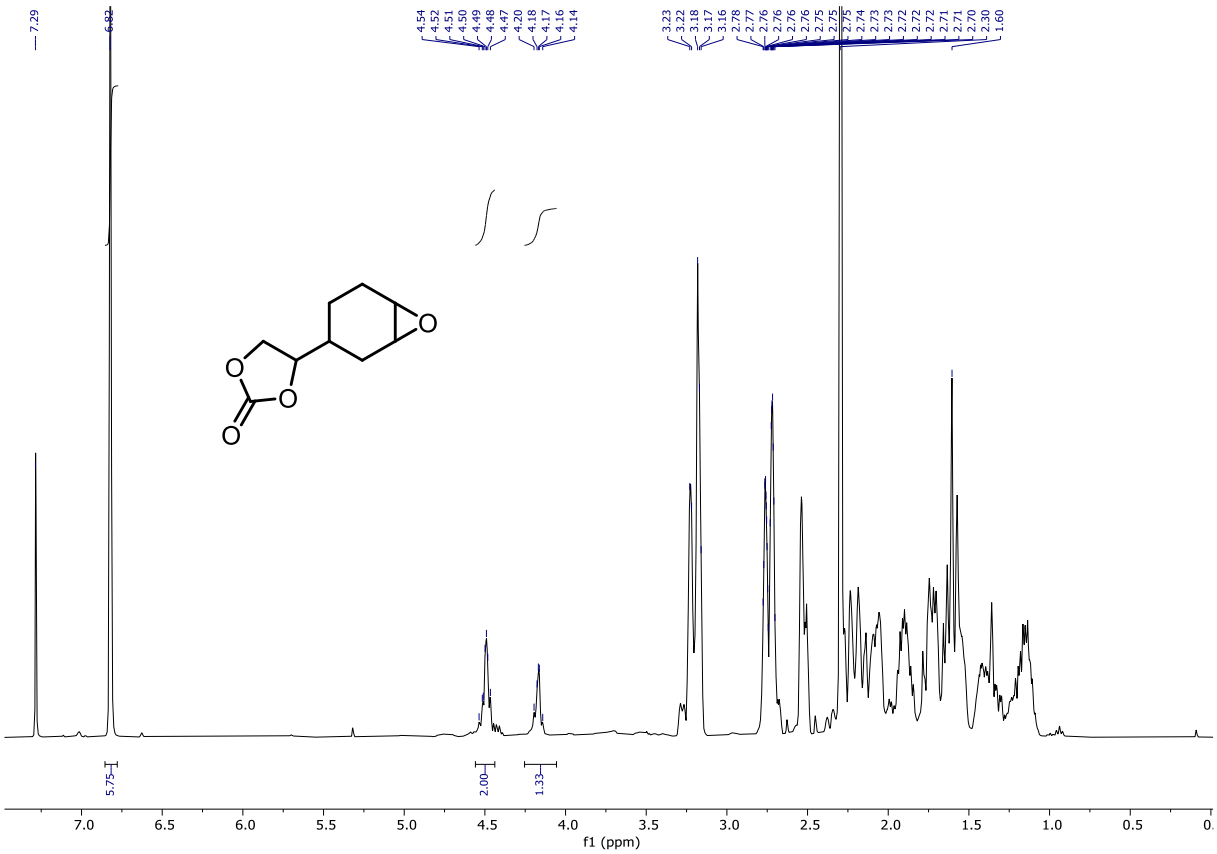

Figure S 49: ^{1}H-NMR spectra of 4-(7-oxabicyclo[4.1.0]heptan-3-yl)-1,3-dioxolan-2-one (reaction crude + mesitylene) in $CDCl_3$

GC Analysis

Yield and conversion of the three substrates used for the screening and optimization of the reaction were calculated by fast GC-FID analysis, with an external calibration method. The calibration curve was determined using dodecane as the internal standard.

Instrumental Parameters.

Column: supelco slb 5ms

Detector: FID

Pressure: 2.64 bar

Total flow = 11.6 mL/min

He flow = 0.34 ml/min

H_2 flow = 40 mL/min

Air flow = 400 mL/min

Split ratio = 30

Propylene oxide and propylene carbonate

In the case of propylene oxide, it was not possible to determine conversion, because the substrate is quite volatile (T_{eb}=34°C) and part of the substrate was inevitably lost by heating and while degassing the autoclave; for the same reason propylene oxide has similar a retention time when compared with the solvents used to dilute the samples and could not be measured by GC analysis. The calibration curve was determined using 4 standard solutions of commercial propylene carbonate (rt = 1.3 min), in a concentration range of 0.35-1 mg/mL, each containing dodecane (rt = 2.03 min) as the internal standard in a concentration of 0.1 mg/mL.

Ramp	Rate (°C/min)	Temperature (°C)	Hold time (min)
injection	-	100	0
1	30	200	3
2	50	230	2

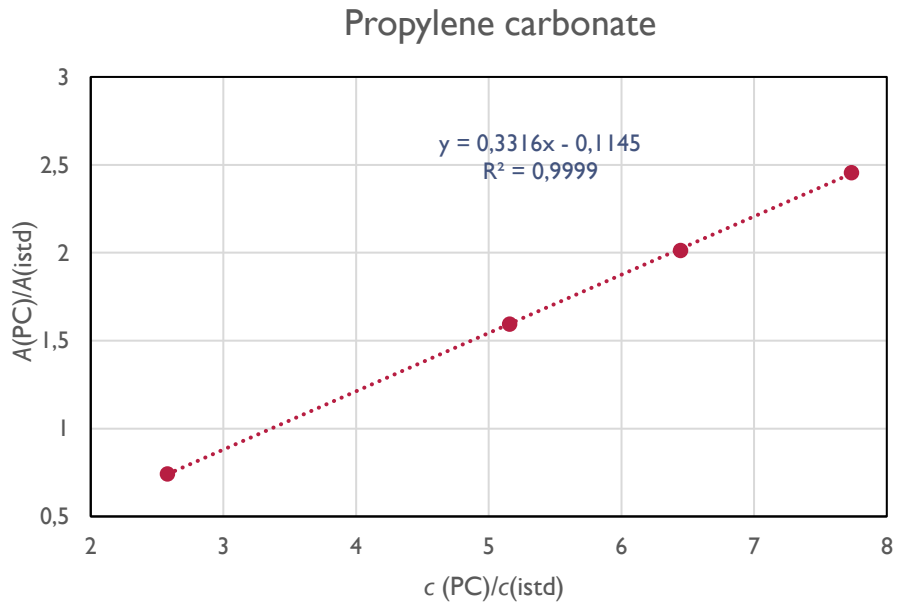

Figure S 50: calibration curve for propylene carbonate. PC concentration = 0.37-0.72-0.92-1.1 mg/mL (rt = 1.3 min), istd concentration = 0.1 mg/mL (rt = 2.09 min)

Styrene oxide and styrene carbonate.

The calibration curve was determined using 5 standard solutions of commercial styrene oxide, in a concentration range of 0.05-0.33 mg/mL, and 5 standard solution of styrene carbonate, in a concentration range of 0.05-0.30, each containing dodecane (rt = 2.03 min) as the internal standard in a concentration of 0.1 mg/mL.

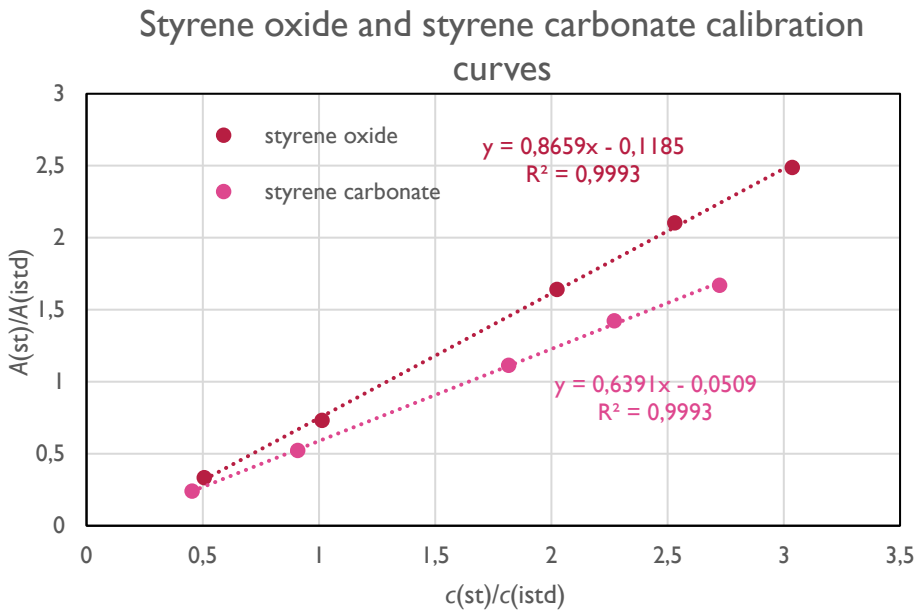

Figure S 51: Calibration curves for styrene oxide and styrene carbonate. SO concentration = 0.05-0.11-0.22-0.27-0.33 mg/mL, SC concentration = 0.05-0.10-0.20-0.25-0.30 mg/mL, istd concentration = 0.1 mg/mL

Cyclohexene oxide and cyclohexene carbonate.

The calibration curve was determined using 4 standard solutions of commercial cyclohexene oxide, in a concentration range of 0.05-0.26 mg/mL, and 4 standard solution of styrene carbonate, in a concentration range of 0.05-0.26 mg/mL, each containing dodecane as the internal standard in a concentration of 0.1 mg/mL.

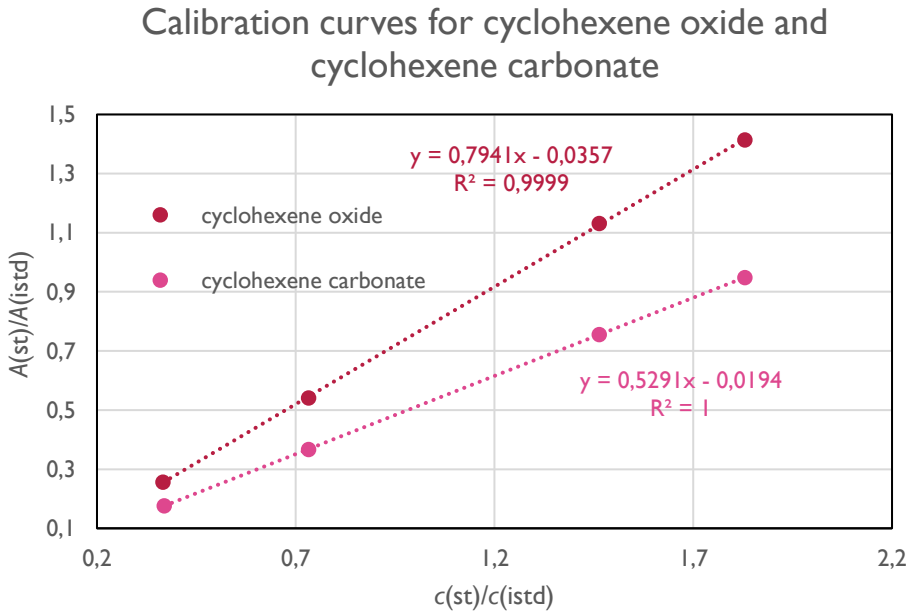

Figure S 52: GC-FID calibration curves for cyclohexene oxide and cyclohexene carbonate. CO concentration = 0.05-0.10-0.21-0.26 mg/mL (rt = 1.58 min), SC concentration = 0.05-0.10-0.21-0.26 mg/mL (rt = 4.31), istd concentration = 0.1 mg/mL (rt = 3.49 min)